Effect of adsorbate's polarity, steric hindrance, aromaticity, and boiling point on competitive adsorption in a multi-staged countercurrent fluidized bed reactor using activated carbon and zeolite

by

Saeid Alizadeh

A thesis submitted in partial fulfillment of the requirements for the degree of

Master of Science

in

Environmental engineering

Department of Civil and Environmental Engineering

University of Alberta

ABSTRACT

Understanding the multi-component adsorption of volatile organic compounds (VOCs) is of essential importance for real-world engineering applications. Various properties of VOCs can affect their competitive adsorption when there is a mixture of these compounds in the process stream. This thesis investigated the effects of polarity, steric hindrance, aromaticity, and boiling point on competitive adsorption of VOCs in a multi-staged countercurrent fluidized bed reactor using beaded activated carbon (Kureha BAC G-70R) and beaded zeolite (ZEOCAT F603). The former is a highly microporous activated carbon, and the latter is a (50:50 wt. %) mixture of ZSM-5 & USY.

Adsorption isotherms were obtained for each VOC on each adsorbent for the concentration range of 50 to 1000 ppm. For the multicomponent tests, four pairs of VOCs (methyl isobutyl ketone (MIBK) and heptane for the polarity effect, hexane and cyclohexane for the steric hindrance effect, p-xylene and octane for the aromaticity effect, and 1,2,4-trimethylbenzene (TMB) and cumene for the boiling point effect) were selected based on their physical/chemical properties and each pair of VOCs targeted a specific factor.

In terms of adsorption isotherms, Kureha BAC G-70R exhibited a remarkably higher adsorption capacity as opposed to ZEOCAT F603 for all the VOCs due to its higher surface area and pore volume. Moreover, the results showed that BAC had the highest affinity for TMB followed by cumene with a slight difference, and hexane and octane showed the lowest adsorption capacity within the entire range of concentration. For the zeolite, the lowest affinity in the entire concentration range was observed for cyclohexane. For the lower range (< 200 ppm), MIBK had the highest adsorption capacity.

Regarding the multicomponent tests, the adsorption capacity of the VOCs was similar when BAC was used as the adsorbent, while the zeolite had a higher adsorption capacity for MIBK which indicated its affinity toward the polar compound. Regarding the effect of steric hindrance, the cyclohexane molecular structure and conformations seem to hinder its adsorption into both adsorbents' pores and as a result, cyclohexane's adsorption capacity was lower compared to hexane on both adsorbents. Further, the aromatic structure of p-xylene may have caused this VOC to have a stronger affinity toward BAC, which led to its higher removal efficiency in the middle stages of the fluidized bed (2, 3, & 4), but not strong enough to impact its overall removal efficiency in comparison to that of octane. The zeolite was not affected by the aromaticity effect and both p-xylene and octane had a similar removal efficiency in the fluidized bed reactor. The difference of approximately 20°C between the boiling point of TMB and cumene did not impact their competitive adsorption. TMB and cumene showed a similar removal efficiency in multicomponent adsorption using both adsorbents. The X-ray photoelectron spectroscopy (XPS) results from Kureha BAC G-70R provided additional explanations for the results from the multicomponent test. Oxygen-containing groups (hydrophilic sites) were detected on BAC surface but, it is assumed that due to the low content of hydrophilic sites, they could not facilitate the adsorption of the polar compound. The graphitic carbon on BAC surface may have caused π-electron donor-acceptor (π-EDA) interactions between the aromatic compound and BAC, and presumably, they promoted p-xylene adsorption in the middle stages of the fluidized bed.

ACKNOWLEDGEMENT

I would like to dedicate this thesis to my beloved and dearest parents, Hossain and

Masoumeh, for this work could not have been done without your boundless love,

motivation, and support.

Table of Contents

LIST OF TABLES

LIST OF FIGURES

LIST OF ABBREVIATIONS AND NOMENCLATURE

AC	Activated Carbon
BAC	Beaded Activated Carbon
BET	Brunauer, Emmett, And Teller Theory
BTEX	Benzene, Toluene, Ethylbenzene, And Xylene
CEPA	Canadian Environmental Protection Act
CFA	Coal Fly Ash
CNT	Carbon Nanotube
DFT	Density Functional Theory
DR	Dubinin-Radushkevich
EPA	Environmental Protection Agency
FAU	Faujasite
FID	Flame Ionization Detector
HCP	Hyper-Crosslinked Polymer
GC-MS	Gas Chromatography – Mass Spectrometry
IAST	Ideal Adsorbed Solution Theory
IUPAC	International Union of Pure And Applied Chemistry
MBR	Moving Bed Reactor
MEK	Methyl Ethyl Ketone
MFC	Mass Flow Controller
MFI	Mobil Five
MIBK	Methyl Isobutyl Ketone
MOF	Metal Organic Framework
NOx	Nitrogen Oxides
POM	Particulate Organic Matter
PAH	Polycyclic Aromatic Hydrocarbons
RH	Relative Humidity

SAC	Spherical Activated Carbon
SMBR	Simulated Moving Bed Reactor
SVOC	Semi-Volatile Organic Compound
TMB	1,2,4-Trimethylbenzene
VOC	Volatile Organic Compound
VSM	Vacancy Solution Model
VVOC	Very Volatile Organic Compound
WHO	World Health Organization
XPS	X-Ray Photoelectron Spectroscopy

Chapter 1:   Introduction and research objective

1.1. Background and motivation

1.1.1   Volatile Organic Compounds (VOCs):

Volatile organic compounds (VOCs) are "carbon-containing gases and vapors" incorporating "one-ring and two-ring (< 1%) aromatic hydrocarbons, aliphatic hydrocarbons, alcohols, ketones, esters, or ethers" (excluding carbon dioxide, carbon monoxide, methane, and chlorofluorocarbons) (Government of Canada, 2013; Lashaki, et al., 2020). According to The World Health Organization (WHO), VOCs are organic compounds with saturated vapor pressure greater than 133.322 Pa and boiling point of 50 to 260 ℃ at atmospheric pressure (Zhu et al., 2020). They are in liquid state at ambient temperature and evaporate readily into the atmosphere. The U.S. environmental protection agency (EPA) ascertained 189 hazardous air pollutants and among them, 97 are known as VOCs. Further, in the Canadian Environmental Protection Act, 1999 (CEPA 1999), Schedule 1 section defines VOCs as toxic compounds (Government of Canada, 2021; Parmar & Rao, 2009).

VOCs are deemed one of the most pervasive environmental contaminants which adversely affect human health and wellness (Khan & Ghoshal, 2000). The common VOCs can be classified into several groups on the basis of their different properties. Based on the boiling point, the VOCs can be classified as very volatile organic compounds (VVOCs), VOCs, and semi-volatile organic compounds (SVOCs) (Zhu et al., 2020).

Two main reasons that VOCs are regulated and of environmental concerns are: 1) toxicity of various VOCs which results in human health problems, and 2) formation of ozone due to the photochemical reaction of VOCs with Nitrogen Oxides (NOx) (Kim, 2011). Considering the health

and environmental concerns, and strict regulations on VOCs emissions, there is a demand for more advanced and efficient control of VOCs emission.

1.1.1.1. *Sources of VOCs*

Volatile organic compounds can be released into the atmosphere from natural sources such as marine and freshwater, soil and sediments, and microbial decomposition of organic material (Guenther, et al., 1995). Anthropogenic sources of VOCs include petroleum storage tanks, painting operations, and oil and gas operations (Khan & Ghoshal, 2000; Kim, 2011). Examples of VOCs containing commercial products include coatings, automotive refinishing products, asphalt, and printing and inks (Government of Canada, 2017).

In the car manufacturing industry, VOCs are primarily produced in the automotive painting section in which coatings are used for vehicles and mobile equipment. Most VOC emissions come from the paint spraying operations (Government of Canada, 2021; Kim, 2011; Papasavva, Kia, Claya, & Gunther, 2001).

VOCs usage as solvents by a car manufacturing company in North America was reported to be roughly 6.58 kg/vehicle (Kim, 2011). Further, as stated by Canada's air pollutant emission inventory, in 2019, roughly 1.7 megatonne of VOCs were emitted in Canada. Contributors to VOCs emission are depicted in **Figure 1.1**. In that year, the oil and gas industry had the largest share of VOCs emission with approximately 40% of the total anthropogenic emissions. The second largest share corresponds to paints and solvents with 18% followed by transportation and mobile equipment with 17%. Commercial/ residential/ institutional, agricultural, and manufacturing are the next contributors with 10%, 7%, and 6%, respectively. Other sources such as ore mining, utilities, fires, and incineration and waste had the least contribution. Moreover, from 1990 to 2019,

the VOCs emissions from paints and solvents has decreased by around 17% (Government of Canada, 2019).

Ore & mineral,
utilities, fires, and
incineration and waste
2%

Manufacturing
6%

Agricultural
7%

Commercial/Residenti
al/Institutional
10%

Oil & Gas Industry
40%

Transportation and
Mobile Equipment
17%

Paints and Solvents
18%
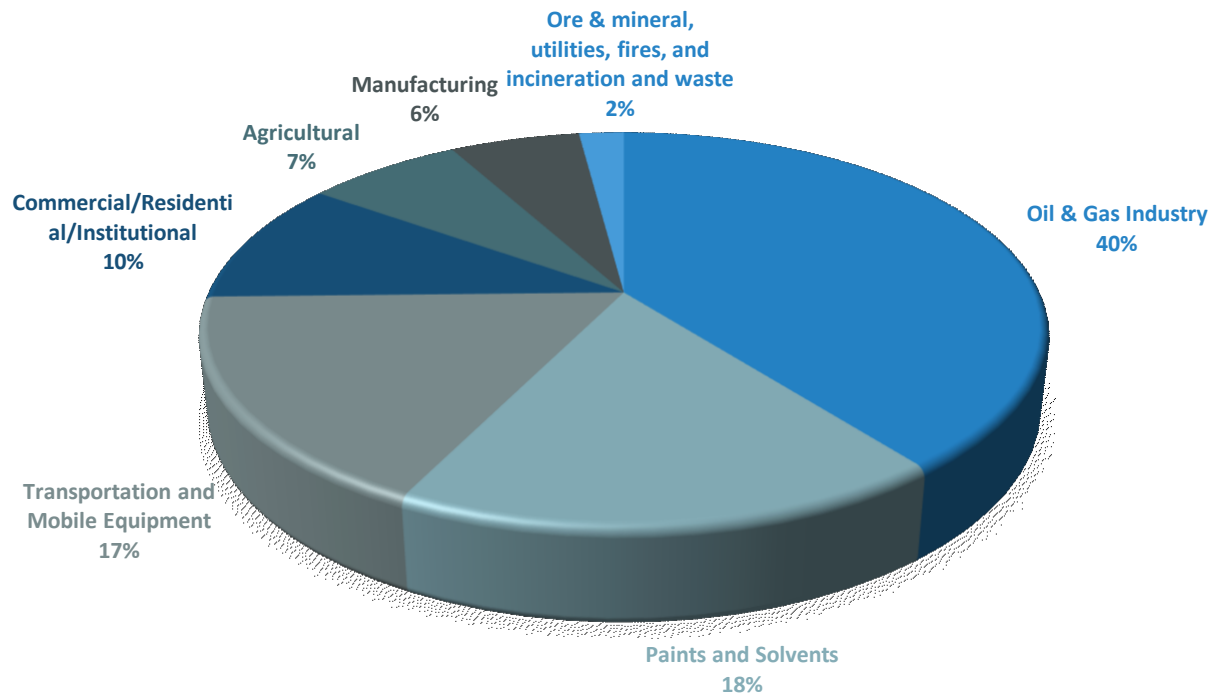
Figure 1.1. Contribution of different industrial sectors to VOCs emission in 2019
(Government of Canada, 2019)

1.1.1.2.   VOCs Impact on human health and the environment

VOCs are the most pervasive air pollutants. Some VOCs can cause damage to kidneys, liver, cardiovascular system, blood components, and intestines. In more severe situations they may impair memory and vision and be fatal (Leslie, 2000; Li, et al., 2020). Some VOCs such as aromatic compounds are carcinogenic (Zhang et al., 2017). For example, benzene is detrimental to bone marrow cells because of its genotoxic and carcinogenic effects (Pariselli et al., 2009) or

exposure to high concentrations of formaldehyde can cause nasopharyngeal cancer (Zhang et al., 2017).

VOCs are the precursor of both ground-level ozone and secondary particulate matter (PM), which are the primary constituents of smog. Ground-level ozone is formed via complex reactions between VOCs and nitrogen oxides (NOx) in sunlight exposure. PM can be formed through reactions involving VOCs, sulphur dioxide, NOx, and ammonia. Numerous health issues are associated with ozone and PM. Based on the risks caused by VOCs, there have been various regulations to reduce their emission and improve the air quality (Government of Canada, 2021). Various techniques are used to reduce the emissions VOCs.

1.1.2. Techniques for VOCs abatement

Numerous types of abatement techniques have been developed to control or destroy VOCs emissions and in general, they are categorized into two groups. The goal in the first group is to modify the industrial processes and equipment and it is the most efficient method. It is carried out by substituting VOCs with other materials and altering the conditions of operations or equipment to prevent VOC formation or volatilization. However, the application of this group is limited since the mentioned modifications are not readily feasible. The second group includes add-on-control techniques which are implemented to either destroy or recover VOCs. They can be classified as destruction and recovery techniques. A summary of several add-on-control methods are listed in **Table 1.1**.

Table 1.1. Add-on-techniques summary

Technique	Removal efficiency (%)	Advantages	Disadvantages
Thermal oxidation	95-99	• High recovery of energy up to 85% (Parmar & Rao, 2009)	• Halogenated compounds might need extra control equipment (Parmar & Rao, 2009) • Ineffective for low concentrations and materials with high combustion point (Khan & Ghoshal, 2000)
Catalytic oxidation	90-98	• Lower energy requirements compared to thermal oxidation (Khan & Ghoshal, 2000) • Suitable for low concentrations or cyclic operations (Khan & Ghoshal, 2000) • Up to 70% energy recovery (Parmar & Rao, 2009)	• Not cost-effective in terms of replacing the catalyst (Khan & Ghoshal, 2000) • The spent catalyst can be a hazardous waste (Khan & Ghoshal, 2000)
Bio-filtration	60-95	• Inexpensive method when the concentration is low (Bansal & Goyal , 2005) • Energy recovery is possible through paint sludge (Kim, 2011)	• Does not allow for fluctuations in pollutants' concentration (Hashisho, et al., 2008) • Slow process (Parmar & Rao, 2009)
Condensation	70-85	• Balancing out the operating cost is possible via the product recovery (Parmar & Rao, 2009)	• High operating cost for low-boiling VOCs (Khan & Ghoshal, 2000) • High maintenance is required (Parmar & Rao, 2009)

5

Absorption	90-98	• Balancing out the operating cost through wastewater product recovery (Parmar & Rao, 2009)	• High maintenance is required (Parmar & Rao, 2009) • Pretreatment of VOCs might be necessary (Parmar & Rao, 2009)
Adsorption			
1) Activated carbon	80-90	• Possibility of VOCs recovery (Parmar & Rao, 2009) • Suitable for low concentrations • Fluctuations in VOCs concentration does not cause a problem (Hashisho, et al., 2008) • Versatile toward various VOCs (Kamravaei, 2014)	• Flammability (Khan & Ghoshal, 2000) • Humidity can reduce the efficiency (Parmar & Rao, 2009)
2) Zeolite	90-96	• Efficient removal up to 90% humidity level (Parmar & Rao, 2009) • High thermal stability (Khan & Ghoshal, 2000)	• High price of zeolites (Parmar & Rao, 2009)

1.1.2.1. *Adsorption*

Adsorption onto activated carbon and zeolite has been widely applied for VOCs removal at low concentrations (less than 10,000 ppm) (Bansal & Goyal , 2005; Fletcher, Yüzak, & Thomas, 2006; Kamravaei, 2014). Adsorption is deemed a well-known and desirable removal method of VOCs and it is commercially widely used because: 1) it is comparatively economical 2) it is suitable for the low range of concentration values 3) it provides the feasibility of recovery and reuse 4) it is flexible in operation, and 5) it is less energy intensive (Ghoshal & Manjare, 2002; Hashisho, Rood, & Botich, 2005; Lashaki, et al., 2016; Parmar & Rao, 2009; Zhu, Shen, & Luo, 2020). Previous researchers have successfully implemented adsorption for a mixture of VOCs using both activated carbon and zeolite (Kamravaei, et al., 2017; Pasti, et al., 2016; Rajabi , et al., 2021). In the real-world application, the emission streams consist of a mixture of VOCs and hence, multicomponent adsorption is of remarkable importance (Rajabi , et al., 2021; Yanxu, Jiangyao, & Yinghuang, 2008). Therefore, adsorption using activated carbons and zeolites is regarded as a well-founded technique for removing VOC mixtures from gaseous streams.

As dealing with a mixture of VOCs is a common issue in real-world engineering processes, further research on the essence of multicomponent adsorption (i.e. effect of properties of VOCs and effect of the adsorbent type) is necessary to obtain more efficient processes.

1.2. Objective

The objectives of this study are as follows:

1- To investigate the effect of polarity, steric hindrance, aromaticity, and boiling point on competitive adsorption of VOCs from a gaseous stream in a multi-staged countercurrent fluidized bed reactor using two different adsorbents (beaded activated

carbon (BAC Kureha G-70R) and zeolite (ZEOCAT F603)). In order to do so, four binary mixtures (methyl isobutyl ketone (MIBK) and heptane, hexane and cyclohexane, p-xylene and octane, and 1,2,4-trimethylbenzene (TMB) and cumene) were made and the mixtures were composed of 100 ppm of each component. The VOCs were chosen based on their physical/ chemical properties and each pair shared the same properties except for the targeted property to be able to study each effect accurately.

2- To evaluate the affinity of the adsorbents toward each VOC individually through adsorption isotherm tests.

3- To determine the effect of competitive adsorption through comparing the removal efficiency of each VOC in the multicomponent tests and the equilibrium adsorption capacity of each VOC at the concentration of 100 ppm obtained from the isotherm tests.

1.3. Thesis outline

This thesis includes 5 chapters. The first one includes the background and goal of the research.

A review on adsorption, multicomponent adsorption, explanations of adsorbents and adsorbate properties and their effect on adsorption, and different types of adsorption reactors are provided in Chapter 2.

Materials and methods to fulfill the goal of this research are included in Chapter 3. Chapter 4 presents the results and provides the corresponding discussion on the obtained data. Finally, Chapter 5 consists of conclusions and recommendations for future work.

Chapter 2:   Literature review

2.1. Multicomponent adsorption

Adsorption is a separation process in which the surface of a solid (adsorbent) is exposed to a gas or liquid (adsorbate) and the adsorbate molecule is attached to the adsorbent surface due to formation of a bond (Rouquerol et al., 1998; Suzuki, 1989; Yang, 1987). It is attained based on steric, kinetic, and equilibrium effect mechanisms (Yang, 1987). Two main categories of adsorption are physisorption and chemisorption. Physisorption is ascribed to proportionately weak interaction forces between the solid and the adsorbate (Van der Waals forces) and it is reversible. Considering the associated molecules, Van der Waals forces are classified into Keesom forces (difference in charge distribution of the molecules), Debye forces (charge distribution inducing via the molecule with permanent dipole moment), and London dispersion forces (the fluctuation in electron cloud of the molecules without dipole moment) (Yihong et al., 2017). Chemisorption, however, includes electron transferring and chemical reactions (two-dimensional), which results in stronger bonds and irreversibility of the process (Bansal & Goyal , 2005).

Adsorption is an exothermic process. The most distinctive difference between physisorption and chemisorption is the adsorption enthalpy. The magnitude of enthalpy for physisorption is roughly 10-20 KJ per mole, whereas for chemisorption the order is normally 40 to 400 KJ per mole. Further, the thickness of the adsorbed phase in physisorption is larger since it is multimolecular while unimolecular adsorption occurs in chemisorption (Bansal & Goyal , 2005). In general, surface reactivity, adsorbate surface area, nature of the adsorbent and the adsorbate, and temperature and pressure of the adsorption affect what type of adsorption occurs (Bansal & Goyal , 2005).

Recently, adsorption has become a widely used technique to separate multicomponent gaseous mixture (Ghoshal & Manjare, 2002). Typically, the focal point of the literature is single component adsorption. However, the emissions from different sectors of the industry (e.g., painting operations) contain a mixture of VOCs which indicates the necessity of understanding multicomponent adsorption to be able to deal with the real-world engineering applications (Rajabi et al., 2021; Yanxu et al., 2008). Adsorbate-adsorbate and adsorbate-adsorbent are the interactions occurring in multicomponent adsorption. The former one is competition for adsorption sites (Tefera et al., 2014). In a mixture, the component with stronger affinity to the adsorbent is adsorbed and can displace the ones with weaker affinity on the adsorbent (Tefera et al. 2014; Lillo-Rodenas et al., 2006).

Many researchers have investigated the multicomponent adsorption of VOCs. Wang et.al (2012) studied the multicomponent adsorption via two mixtures of two alkanes and eight VOCs in a fixed-bed of activated carbon configuration and displacement of VOCs with lower boiling point by VOCs with higher boiling point was observed. They also reported that in competitive adsorption, the effluent concentration of the weaker component exceeds its inlet concentration due to the displacement by components with stronger affinity.

Kamravaei et.al. investigated multicomponent adsorption in both fixed and single-staged fluidized bed reactors containing activated carbon. In fix bed reactors, heel formation is affected by competitive adsorption because of non-uniform distribution of heavy adsorbates. They also reported that the fluidized bed adsorber showed a 30% decrease in heel buildup compared to the fixed bed reactor. The difference in heel buildup between the reactors are correlated to mixing in the fluidized bed reactor which results in uniform distribution of adsorbates and minimization of competitive adsorption for the multicomponent adsorbates (Kamravaei, et al., 2017).

Rajabi et.al conducted a study on both single- and multi-component adsorption of the emission from crude oil sites which contained a mixture of aromatic and non-aromatic VOCs using two different biochars. They reported the primary mechanisms of both kinds of adsorption as hydrogen bonding, electrostatic interaction, and pi-stacking, and partitioning (Rajabi , et al., 2021).

Nevertheless, there is a need for more investigation on multicomponent adsorption in terms of adsorbate's properties effect and the use of different adsorbents such as zeolites.

2.2. Adsorbents for the adsorption of VOCs

Generally, a wide range of porous materials have been investigated for the adsorption of VOCs, including, carbon-based materials, zeolites, polymeric adsorbents, metal organic frameworks (MOFs). regarding several factors such as capacity, hydrophobicity, thermal stability, and regeneration potentiality. The distinctive features of adsorbents are pore volume, pore size distribution, and surface area. Generally, microporous materials are used in gaseous adsorption. As estimated by the US EPA, the most common adsorbents are activated carbon, zeolites, and organic polymers (Long et al., 2011; Yang., 1987; Zhu et al., 2020).

According to the International Union of Pure and Applied Chemistry (IUPAC), the pores in adsorbents are categorized based on their diameters as shown in **Table 2.1** (Yang, 1987).

Table 2.1. Categories of pores in adsorbents

Pore category	Diameter size
Micropore	Less than 2 nm
Mesopore	Between 2 to 50 nm
Macropore	More than 50 nm

2.2.1. Activated Carbon

Adsorption of VOCs onto carbon materials is a commonly used process and physical adsorption has been introduced as their adsorption mechanism. Activated carbon (AC), biochar, graphene, and carbon nanotubes (CNT) are examples of carbon-based adsorbents (Bansal & Goyal , 2005; Khan & Ghoshal, 2000).

AC is the most widely used adsorbent since it is versatile and has a variety of applications owing to its large surface area, high porosity, and cost-effectiveness. Also, AC provides high removal efficiency at lower concentrations and a high ability to adsorb VOCs. Common precursors for commercial ACs are carbonaceous materials such as wood, coal, nutshells, sawdust, and peat. AC comes in various forms such as powder, spherical, granular, fibrous, and cloth. Spherical activated carbons (SACs) are very popular in gas phase adsorption processes because of their high mechanical strength, minor ash content, great wear resistance, and high micropore volume (Bansal & Goyal , 2005; Chiang et al., 2000; Hung & Lin, 2007; Khan & Ghoshal, 2000; Romero-Anaya et al., 2010; Romero-Anaya et al., 2020).

AC are primarily prepared through the pyrolysis of carbonaceous materials (temperatures < 1000℃). There are two main steps of ACs' preparation. First, is the carbonization of raw materials (temperatures < 800℃ and an inert atmosphere), and second, activation of the produced materials (temperatures between 950 and 1000℃). In addition to carbon, which is the main element of ACs in their structure, they contain hydrogen, nitrogen, sulfur, and oxygen. The surface functional groups and structure of their pores depend on the precursor materials and activation technique, and activation conditions, namely, temperature and oxygen concentration (Bansal & Goyal , 2005; Boulinguiez & Le Cloirec, 2010).

Adsorption of VOCs via activated carbon has been studied by various researchers. Romero-Anaya et.al investigated ethanol adsorption on spherical AC (Romero-Anaya et al., 2015). Yang et.al investigated the adsorption of toluene via five types of AC (Yang, et al., 2018). Wang et.al studied the multicomponent adsorption via two mixtures of two alkanes and eight VOCs with beaded activated carbon (BAC) in a fixed-bed system configuration and the occurrence of competitive adsorption due to the difference in VOCs boiling point was reported (Wang, et al., 2012). Zhu et al. also prepared a comprehensive critical review on adsorption of VOCs with various porous materials (Zhu et al., 2020).

2.2.2. Zeolite

Zeolites are widely used, non-flammable alternatives to activated carbon that possess crystalline aluminosilicate framework with interconnecting voids and fixed pore distribution (Blocki, 1993; Khan & Ghoshal, 2000; Zhu et al., 2020). Zeolites have been popular because of their catalytic properties. They are inorganic substances whose thermal stability, hydrophobicity, acid site density, and acid resistivity can be evaluated by Si/Al ratio in their framework. Zeolites are also referred to as molecular sieves since they can offer selectivity toward adsorbates. These adsorbents can have interconnected uni-, bi-, or tridimensional channels with large internal surfaces. The structural formula of zeolites is $A_{(x/q)}[(AlO_2)_x(SiO_2)_y]n(H_2O)$ in which A could be Ca, Na, K, and other cations (Amdebrhan, 2018; Khan & Ghoshal, 2000; Diaz et al., 2004; Shwanke et al., 2012; Zhu et al., 2020).

Zeolites' specific adsorption sites would induce polar affinity and their pore size ranges from 8 to 20 nm. Their "pore opening size" depends on specific units which are knowns as MR (membered rings). Zeolites' framework topology is described with 3-letter words, for example,

MFI (zeolite ZSM-5) or FAU (zeolites Y). Depending on their Si/Al ratio they fall into three categories of low silica (≤ 2), intermediate silica (2 to 5), and high silica (≥ 5). Higher Si/Al ratio amount in zeolites results in less affinity toward polar compounds (Calleja et al., 1998; Diaz, Salvador et al., 2004; Guth & Henri, 1999; Shwanke et al., 2012).

Pore volume, active sites, and hydrophobicity are some of the factors affecting adsorption onto zeolites (Blocki, 1993). Adsorption of VOCs via zeolites has been researched extensively. Zhou et al investigated the adsorption of benzene vapor on several zeolites developed from coal fly ash (CFA) and they showed the capability of zeolites for VOCs removal (Zhou et al., 2014). Zaitan et al. utilized a hydrophobic zeolite (ZSM-5) for toluene removal. They reported both the suitability of ZSM-5 for the adsorption of toluene and the compatibility with Langmuir isotherm (Zaitan et al., 2016). Amdebrhan investigated the performance of an activated carbon and zeolites (ZSM-5, USY, and 50:50 wt.% of ZSM-5 & USY) for the adsorption of two types of VOCs. They reported a low affinity of water vapor for activated carbon while for three of the zeolites, water adsorption was noticeable which indicated their hydrophilicity and higher affinity toward polar compounds (Amdebrhan, 2018).

2.2.3. Polymeric adsorbents

Organic polymers comprise non-metallic elements such as C, H, O, N, and B and have significantly lower density than other adsorbents. Two main categories of them are hyper-crosslinked polymer (HCP) and macroporous polymer. HCP has attracted interests for the removal of organic compounds from industrial effluent streams (Wang et al., 2013; Wu, et al., 2015; Zhu et al., 2020).

HCP, in particular, has drawn considerable attention for VOCs removal because of their high specific areas and large volume of pores, exclusion of surface functional groups, and hydrophobicity under humid conditions (Zhu et al., 2020). However, the process of synthesizing organic polymeric adsorbents is complicated which reduces their popularity since it cannot be readily implemented in large-scale operations (Zhu et al., 2020).

2.2.4. Metal organic frameworks (MOFs)

Hoskins and Robson introduced metal organic framework, which is a new class of crystalline hybrid porous materials for the first time (Hoskins & Robson, 1989; Zhu et al., 2020). They are built via metal ions or clusters and coordinated with organic ligands and can exist as one-, two-, or three-dimensional structures in an ordered manner (Silva et al., 2015).

In comparison to polymers, MOFs typically manifest everlasting porosity, higher thermal stability, and robustness in structure (Silva et al., 2015). The available metal sites on their pore surface are suitable for VOCs removal (Zhu et al., 2020). Having said that, MOFs have weak dispersive forces because of owning a plethora of void spaces. Besides, the high cost of their preparation makes them an undesirable option for removal of VOCs (Sampieri, et al., 2018).

2.3. Adsorption isotherm

An isotherm is a curve which demonstrates the equilibrium adsorption capacity of an adsorbate on a specific adsorbent at different relative pressures/ concentrations given a constant temperature (Limousin, et al., 2007). Adsorption isotherms can provide the most useful and

essential data on adsorption systems (Pui et al., 2018). Isotherms are affected by the adsorbed species, adsorbate, adsorbent, and various physical properties including temperature. In addition, they define the interaction mechanisms between the adsorbate and the adsorbent (Al-Ghouti & da'ana, 2020).

As stated by the IUPAC organization, the adsorption isotherms can be classified into six groups which are shown in **Figure 2.1** and the description of each type is summarized in **Table 2.2** (Keller & Staudt, 2005).
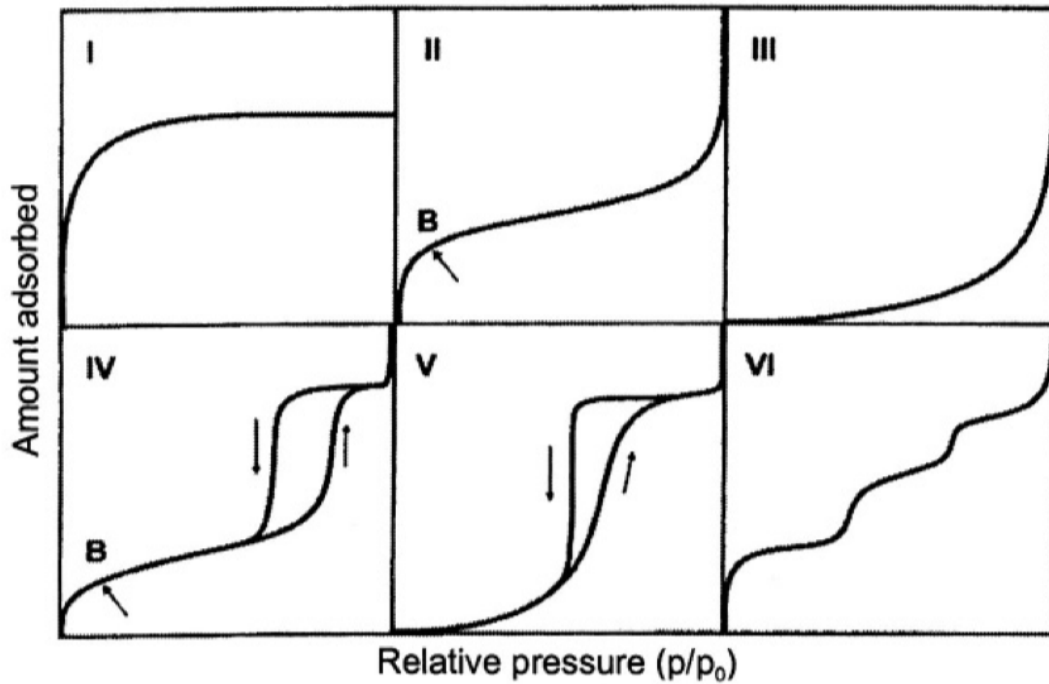
Figure 2.1. Types of isotherms (Al-Ghouti & da'ana, 2020; Keller & Staudt, 2005**)**

Table 2.2. Types of isotherms and their description ((Al-Ghouti & da'ana, 2020; Bansal & Goyal , 2005; Keller & Staudt, 2005; Rouquerol et al., 1998)

Type	Description	Example	References
I	For reversible and monolayer adsorption using microporous adsorbents indicating micropore filling. It can be defined by Langmuir equation.	• Water vapor on zeolite • Hydrogen on charcoal	(Al-Ghouti & da'ana, 2020), (Keller & Staudt, 2005), (Rouquerol, Rouquerol, & Sing, 1998)
II	For adsorption at low pressure, on mesoporous monolayer materials and adsorption at higher pressure near saturation multilayer adsorption and pore condensation.	• Non-polar organic compounds on primarily mesoporous activated carbons	(Al-Ghouti & da'ana, 2020), (Keller & Staudt, 2005)
III	For adsorption processes in which the adsorbate-adsorbate interaction effect is larger compared to adsorbate-adsorbent	• Water on AC and hydrophobic zeolite • Nitrogen on silica gel	(Al-Ghouti & da'ana, 2020), (Keller & Staudt, 2005)
IV	For the adsorption on porous materials whose pore radius size is in the range of 15-1000 Angstroms (Å). Related to particular mesoporous adsorbents indicating pore condensation	• Water vapors on specific types of activated carbon • Benzene on silica gel	(Bansal & Goyal , 2005), (Keller & Staudt, 2005)
V	For the adsorption of both polar and non-polar adsorbates on mesoporous or microporous adsorbents only in case of existence of weak adsorbent-adsorbate interactions.	• Water on carbon molecular sieves • Water on activated carbon fiber	(Al-Ghouti & da'ana, 2020), (Bansal & Goyal , 2005)
VI	For stepwise layer by layer adsorption. The layers are more noticeable in low temperatures	• noble gases on the surfaces of planar graphite • Methane on MgO	(Al-Ghouti & da'ana, 2020), (Rouquerol, Rouquerol, & Sing, 1998)

Many quantitative models have been developed in order to describe and simplify the adsorption process for different adsorbates and adsorbents.

The Langmuir isotherm equation, which is the basis of all the newer developed models, is shown below. This model was originally introduced for the adsorption of gases on a solid adsorbent, and it is applicable for both physical and chemical adsorption. Further, it is consistent with Henry's law at low concentration ranges (Langmuir, 1916; Al-Ghouti & da'ana, 2020; Bansal & Goyal , 2005; Laskar & Hashisho, 2020).

$$q_e = \frac{q_m bC}{1 + bC}$$

Where q_m is the adsorbent maximum equilibrium capacity (kg/kg), q_e is adsorbent equilibrium capacity (kg/kg), C is bulk gas phase concentration (kg/m^3), and b is the temperature dependent Langmuir affinity coefficient (m^3/kg).

This model was developed using certain assumptions of which the most important ones are:

1) The adsorbed particles are accommodated on specific sites on the surface of the adsorbent

2) Each site seats merely one adsorbed molecule

3) Rates of adsorption and desorption are equal

4) All sites are energetically equivalent.

Another isotherm model, which is empirical and describes reversible and non-ideal adsorption, is Freundlich isotherm. This model is used for modeling of VOCs' adsorption as well (Bansal & Goyal , 2005; Laskar & Hashisho, 2020).

$$q_e = K_f C^{\frac{1}{n}}$$

Where K_f and n are constant values for a specific pair of adsorbent and adsorbate. n is indicative for the degree of heterogeneity of the adsorbent's surface. In contrast to Langmuir isotherm, Freundlich model considers a multilayer adsorption (Al-Ghouti & da'ana, 2020; Benkhedda et al., 2000; Laskar & Hashisho, 2020).

The other model useful for heterogenous gas-solid systems is Brunauer-Emmett-Teller (BET) isotherm. It takes into account the same assumptions as Langmuir model, but it considers a multimolecular adsorption via generalizing "Langmuir treatment of unimolecular adsorption." That is to say, in the formation of multiple layers of molecules, the first layer will be a base for the adsorption of the second layer and so on, and the interactions between molecules are not taken into account (Bansal & Goyal , 2005; Brauner, Emmett, & Teller, 1938).

To describe the mechanism of adsorption on heterogenous surfaces with Gaussian energy distribution, Dubinin-Radushkevich (DR) adsorption is used. Typically, the DR model is implemented for gas adsorption on activated carbon and zeolites, and since the core of this model is thermodynamics, it is well-founded and reliable (Al-Ghouti & da'ana, 2020; Laskar & Hashisho, 2020). Hung et al conducted a study on predicting the adsorption capacity of nine aromatic and chlorinated VOCs on two different activated carbons using the D-R-L model which was obtained through the integration of DR and Langmuir equations. They reported that DR model overestimated the adsorption capacity for low relative pressure ($< 1.5 \times 10^{-3}$) and they attributed this weakness to the deviation of the DR model from Henry's law at low pressures.

Moreover, for multicomponent adsorption several models have been developed. Jain and Snoeyink's extended Langmuir isotherm, which considers the competitive adsorption with an exclusive factor (Jain & Snoeyink, 1973). Other examples of multicomponent isotherm models include ideal adsorbed solution theory (IAST) which is based on solution thermodynamics and

Raoult's law with specific assumptions and it has been successfully implemented for multicomponent competitive equilibria of VOC mixtures (Myers & Prausnitz, 1965), and vacancy solution model (VSM) proposed by Suwanayuen and Danner with the assumption of vacancies and two solutions (gas phase and adsorbed phase) for the system (Suwanayuen & Danner, 1980),

2.4. Adsorbate properties

Physical and chemical properties of the adsorbates, namely, boiling point, polarity, and molecular weight can influence the multicomponent adsorption processes. Rajabi et. al. reported the governing mechanisms in competitive adsorption of VOCs such as the VOC's molecular size and shape, VOC's molecular weight, electrostatic attraction, functional groups, and "partitioning into non-carbonized mass" (Rajabi , et al., 2021). When microporous adsorbents are at use, molecular shape selectivity, which is the preference of the adsorbent toward a specific adsorbate because of the size and shape, is a determinant factor for adsorption. For instance, it is widely known that linear hydrocarbons are adsorbed more compared to their branched isomers due to the steric hindrance effect. Further, aromaticity has been recognized as a factor impacting adsorption since the aromatic rings reinforce the π-π interaction between the adsorbent and the adsorbate. (Bell et al., 2011; Bozbiyik, et al., 2014; Lin & Xing, 2008; Ouzzine et al., 2019).

2.4.1. Polarity

The available sites on activated carbons can be hydrophobic or hydrophilic and therefore, polarity of the adsorbate is one of the influential factors on adsorption. For instance, oxygen-containing surface functional groups on activated carbons are one of the main contributors for hydrophilic VOCs adsorption. Further, zeolites possess specific sites on the surface and exhibit

strong affinity toward polar compounds mostly due to the local electrostatic forces in their framework (Meng et al., 2019; Monneyron et al., 2003; Rodriguez-Reinoso et al., 1992; Rouquerol et al., 1998).

Meng et al studied the adsorption of VOCs using activated carbon fiber and they observed the key role of polarity of the adsorbates. Methanol and acetone were preferably adsorbed on the polar groups of the adsorbent as a result of dipole-dipole interactions (Meng et al., 2019; Shen et al., 2008). Lee at al. carried out single- and multi-component adsorption of toluene and acetone using activated carbon. A higher adsorption of toluene was reported due to the hydrophobicity of the AC and non-polarity of toluene. Lower adsorption of acetone was correlated to the difference between the AC and acetone polarity (Lee et al., 2006). Rodriguez-Reinoso et al prepared an activated carbon with an attempt to minimize the oxygen groups on the surface and they observed a higher adsorption of nitrogen gas because of its non-polarity (Rodriguez-Reinoso et al., 1992). Ouzzine et al. also observed the affinity of spherical activated carbon, with low surface oxygen groups, for benzene with a low polarity (Ouzzine et al., 2019). The significance of adsorbates' polarity for adsorbent's selectivity was reported by Calleja et. al based on single- and multicomponent adsorption experiments of pure carbon dioxide, ethylene, and propane on three zeolites with different Si/Al ratio. They observed higher adsorption for the molecules with higher quadrupole moment by zeolites with the least amount of Si/Al ratio (Calleja et al., 1998).

2.4.2. Steric hindrance

Huddersman and Klimczyk observed the steric hindrance effect during the separation of branched hexane isomers using zeolites since parts of the zeolites were not accessible to the more branched hydrocarbons (Huddersman & Klimczyk, 1996). Multicomponent adsorption of toluene,

methyl ethyl ketone (MEK), and 1,4-dioxane on zeolites was studied by Monneyron et al. and less adsorption of toluene was observed in binary mixtures due to the steric hindrance effect (Monneyron et al., 2003). Lashaki et al. investigated the adsorption of organic compounds onto activated carbon and reported pore blockage of the activated carbon by the bulky compounds (Lashaki, et al., 2012). Molecular simulation and experimental study of cyclohexane adsorption on various zeolites was carried out by Slawek et.al. and they reported the impact of cyclohexane molecules and conformations on its adsorption into the pores of different zeolites frameworks such as MFI and FAU (Slawek et al., 2018).

2.4.3. Aromaticity

The compounds with aromatic structure can be adsorbed on the surface of carbon via π-π stacking, electrostatic attraction, functional groups, and partitioning into the non-carbonized portion if the carbonaceous adsorbent contains a considerable non-carbonized mass. It can be suggested that the adsorption of p-xylene is driven by the interaction of π electrons existing in its benzene rings "with the π electrons displaced on the carbon's surface". Activated carbons exhibit strong affinity toward aromatics and the adsorption of compounds with a simple aromatic-ring structure on ACs is higher than the aromatic chemicals with side chains. Further, adsorption of aromatics on microporous zeolites has been investigated for separation and catalysis processes. The structure of certain zeolites is uniform and polar, and the adsorption of aromatics on polar zeolites is a "polarity-induced phenomenon" (Lachet et al., 1999; Paredes-Doig et al., 2014; Rajabi , et al., 2021; Wang et al., 2004). The effect of aromaticity was observed by Lin et al by experimenting with multiple VOCs adsorption using carbon nanotubes. They reported an increase in the adsorption of components with a higher number of aromatic rings. The adsorption of the compound with no aromatic ring occurred without π-π interaction and only due to the hydrophobic

force, which is the interaction of the non-polar VOC with the adsorbent's hydrophobic sites (Lin & Xing, 2008). Tang et al studied the adsorption of aromatic compounds on graphene oxide and the main factor influencing the adsorption capacity was found to be the π-stacking ability (Tang, et al., 2018). Dispersive and electrostatic interactions were reported as the main mechanisms of the adsorption of aromatic compounds on activated carbon by Villacanas et al (Villacañas et al., 2006). The adsorption of aromatic compounds via three different adsorbents (activated carbon, 13X zeolite, and silica gel) was investigated by Wang et al. (Wang et al., 2004). The structure of the adsorbents was highly influential on the adsorption and in general, activated carbon showed higher adsorption capacity compared to the other two adsorbents (Wang et al., 2004).

2.4.4. Boiling point

Physisorption of an adsorbate on porous materials resembles vapor-liquid phase transitions, and in the adsorption process, compounds with higher boiling point are preferred to the compounds with lower boiling points. Further, "liquid-like condensation" plays a part in the adsorption of VOCs on an adsorbent. Hence, the boiling point of VOCs are deemed to be important in their adsorption behavior (Chiang et al., 2001; Zhang et al., 2017). Higher boiling point in a VOC leads to having a stronger affinity with the adsorbents and as a result, VOCs with a higher boiling point can replace those with a lower boiling point during multicomponent adsorption (Zhang et al., 2017).

Giraudet et al. investigated the adsorption of dichloromethane, ethanethiol, and siloxane D4 with boiling points of 39.6, 35 and 176 ℃ on activated carbon fibers. They reported a similar adsorption capacity for dichloromethane and ethanethiol, while siloxane D4, the compound with a higher boiling point, was reported to have a higher adsorption capacity (Giraudet et al., 2014).

Dobre et al. also reported a higher saturation adsorption capacity for VOCs with higher boiling points (Dobre et al., 2014).

Wang et. al studied the adsorption of a mixture of VOCs on beaded activated carbon. They observed competitive adsorption between compounds and reported the displacement of the compounds with lower boiling point by the compounds with higher boiling point. The components with lower boiling point showed higher outlet concentration than the inlet value in the breakthrough curve which indicated their displacement. It is noteworthy that the boiling point was suggested as only one of the impacting factors on adsorption (Wang, et al., 2012).

2.5. Bed configuration

Three common adsorption bed configurations for both industrial and experimental purposes are: 1) fixed bed, 2) moving bed, and 3) fluidized bed reactors. The configuration of the bed is a determinant factor for evaluation of adsorption capacity and irreversibility.

2.5.1. Fixed bed reactor

Fixed bed reactors are typical in gas adsorption processes and several parameters such as temperature, adsorbate concentration, adsorbent amount and flow rate are important in fixed bed system adsorption. A satisfactory performance of the adsorption bed is obtained depending on the even distribution of gas within the fixed bed. Further, since adsorption is an exothermic process, the produced heat might lead to the creation of hot spots across the bed which consequently might cause thermal oxidation of the carbonaceous adsorbent and fire hazards. Channeling or clogging may also occur which decreases the efficiency of the fixed bed adsorption. There is also a higher

probability of undesirable by-product development in fixed bed systems (Pui et al., 2018; Yang W.-C. , 2003; Yazbek et al., 2006).

2.5.2. Moving bed reactor

The first moving bed reactor (MBR) was patented by Andrews in 1890 (United States of America Patent No. 426092, 1890). A MBR is a reactor in which granular adsorbents are continuously in motion throughout the bed and regenerated in a specific unit. MBRs have been used in gas separation sections, The application of moving bed in removal of VOCs was suggested and it was reported that MBR was useful in addressing the carbon attrition and flow blockage problems (Larsen & Pilat, 1991).

2.5.3. Fluidized bed reactor

When a fluid (typically a gas) is flowed through a bed of particles, it passes through the void spaces while the particles stay motionless. If the fluid flow rate increases, the drag force also increases which eventually leads to the movement of the particles and expansion of the bed. At this point, the particles are considered "fluidized", and this system which is similar to a fluid is called a fluidized bed (Kunii & Levenspiel, 1991; Van lare, 1991; Yates & Mullin, 1983). Fluidized bed reactors offer several benefits compared to fixed bed systems which are presented later on in this study. They are used in a variety of industrial units such as petroleum, pharmaceutical, metallurgical, energy, and drying (Kunii & Levenspiel, 1991; Saxena & Vadivel, 1988). In terms of the utilized adsorbents in fluidized beds, SACs are widely implemented since they are readily fluidized, and exhibit low attrition and low pressure drop (Romero-Anaya et al., 2010; Wang, et al., 2009).

The velocity of gas at which the fluidization of the bed can occur, can be determined based on the pressure drop throughout the bed. The velocity at which the particles are floating, and the pressure drop is equal to "the weight of the bed per unit area" is the minimum fluidization velocity (U_{mf}) (Van lare, 1991; Yates & Mullin, 1983). There are different classifications of regimes in fluidized beds, but they can broadly be classified into smooth (particulate) and aggregative (bubbling). In the particulate regime, uniform scattering of solids without distinguishable bubbles takes place (Yang W.-C. , 2003). The emergence of bubbles (bubbling regime) occurs when the bed velocity becomes greater than the minimum fluidization velocity. The velocity at which bubbles appear in the bed is called the minimum bubble velocity (U_{mb}). In the industry, the reactors are frequently operated in the bubbling regime in which the fluid velocity is generally 5-30 times higher than U_{mf}. (Inglezakis, 2006; Philippsen et al., 2015; Van lare, 1991).

Factors such as air flow rate (superficial gas velocity), weir height, and adsorbent feed rate affect fluidized beds efficiency. According to Roy et.al., higher adsorbent (solid) feed rate and lower air flow rate were demonstrated to enhance the CO_2 removal in a three-staged fluidized bed. Mohanty and Meikap also showed a constant pressure drop for all the stages in the bed with a 2% deviation (Roy, Mohanty, & Meikap, 2009).

Varying parameters such as the characteristics of the adsorbent particles play a key role in determining the fluidization behavior and the overall removal efficiency of the adsorption system (Davarpanah, 2020; Geldart, 1973; Philippsen et al., 2015; Van lare, 1991). The acknowledged categorization of particles which was introduced by Geldart is demonstrated in **Table 2.3** (Geldart, 1973). Regarding the group A, the transition from the particulate fluidization regime (the regime before bubbling) to the bubbling regime occurs rapidly as gas velocity increases (Davarpanah, 2020).

Table 2.3. Geldart categories of powders

Group	Characteristics
A	• Small size ($30 < d_p < 150\ \mu m$) and/or low particle density • Readily fluidized • Maximum size of bubbles occurs • A better control on bubbles speed and growth is achievable • The possibility of homogenous expansion
B	• Relatively larger particles ($40 < d_p < 500\ \mu m$) and density ($1.4\text{-}4\ \text{g/cm}^3$) • Readily fluidized • Marginally higher velocity than minimum fluidization velocity is needed for bubbles to form • Minimum fluidization velocity is approximately equal to minimum bubbling velocity (bubbles appear roughly as soon as the fluidization starts)
C	• Very small particles ($d_p < 30\ \mu m$); cohesive • Fluidization occurrence is hard • Mechanical stirrers may facilitate fluidization • The possibility of channeling
D	• Large particles ($d_p > 500\ \mu m$) • Hard to fluidize • Non-uniform fluidization • Comparatively poor solids mixing

Fluidized bed systems have the advantages of high mass transfer between gas and solid and more readily controllable in large scale operations. They also provide excellent temperature control while being implemented for gas purification and separation processes because of the high intensity mixing of solid particles and air in the bed (Davarpanah, 2020; Mohanty et al., 2009).

It is noteworthy that horizontal screens in the fluidized bed stages decrease the creation of bubbles and limits the axial mixing of the phases, and consequently, the efficiency of the bed can increase (Varma, 1975). A coherent process is attainable via staging as well since it can minimize the extensive residence time distribution of the solids in fluidized beds (Davarpanah, 2020).

Furthermore, comprehending all the controlling parameters in a fluidized bed operation and their effects is an obstacle. Adsorption in a fluidized bed is based on factors such as fluid dynamics, mass transfer, and heat transfer (Davarpanah, 2020).

2.5.3.1.   *Advantages and disadvantages*

The advantages and disadvantages of fluidized bed reactors can be defined in comparison to fix bed reactors. Having a higher degree of agitation is the primary reason for the operational advantages of fluidized bed reactors, however, it might cause several issues. The advantages and disadvantages of fluidized bed reactors are summarized in **Table 2.4**.

Table 2.4. Advantages and disadvantages of fluidized bed reactors

Advantages	Disadvantages
• Providing lower heel buildup compared to fixed-bed systems (Kamravaei, et al., 2017) • Mass transfer coefficient is higher in fluidized bed reactors which results in better overall mass transfer (Yazbek et al., 2006). • Immense heat transfer in fluidized bed reactors between particles and gas leads to a better temperature control (Yazbek et al., 2006). • Fluidized bed reactors prevent the creation of "hot spots", and the bed is operated in an isothermal mode (Hamed et al., 2010). • Thanks to the fluidization phenomenon, fluidized bed reactors provide the ability to regenerate the adsorbents continuously (Davarpanah, 2020).	• Pipes and internal parts of fluidized bed are susceptible to erosion because of the high agitation and breaking up of the bubbles inside the bed (Davarpanah, 2020; Missen et al., 1999). • The attrition of solids may require recovery equipment and recurrent maintenance (Missen et al., 1999). • If large bubbles are created, they can hinder the contact between solids and the fluid which leads to a decrease in the process efficiency. This issue could be alleviated via using a multi-staged fluidized bed (Missen et al., 1999; Davarpanah, 2020) • It is more complex to predict the fluidized bed reactors' behavior. Consequently, designing, scaling up, and operating fluidized beds are more complicated (Davarpanah et al., 2020).

• The fluidized bed reactors are extremely useful in case of dealing with large quantities of solid substances (Yates & Mullin, 1983). • The fluidized bed reactors allow lower pressure drops across the bed (Kamravaei, 2014). • Significant interface area between gas and solids and mixing of the particles (Rüdisüli et al., 2012). • High efficiency in terms of operation and consuming low energy (Rüdisüli et al., 2012). • Fluidized bed reactors are suitable for dealing with large flow rates (Davarpanah et al., 2020). • Fluidized beds reactors exhibit the features of reactions with low temperature and adequate reaction time (Mohanty & Meikap, 2011)	• Wide residence time distribution of the solid particles which can be minimized with implementing countercurrent multi-staged beds (Roy et al., 2009).

2.5.3.2. *Application of fluidized bed reactors in adsorption*

Several studies have investigated the adsorption of organic and non-organic adsorbates in fluidized bed reactors. Chiang et.al conducted research on the performance of the fluidized bed reactor using activated carbon as the adsorbent and polycyclic aromatic hydrocarbons (PAHs) and benzene, toluene, ethylbenzene, and xylene (BTEX) and particulate from flue gas of an incinerator. They reported a high removal efficiency of the fluidized bed reactor for PAHs and BTEX. They also concluded that as the adsorption temperature rises, the fluidized velocity rises too, and it leads to a higher removal efficiency of particles in flue gas (Chiang et al., 2000).

Hamed et. al investigated the adsorption of humidity via both fixed and fluidized bed reactors to compare their performance and reported that due to the higher mass transfer rate in the fluidized bed, removal efficiency was 20% higher than the fixed bed (Hamed et al., 2010). Davarpanah et al. also studied the adsorption of 1,2,4-trimethylbenzene on a beaded activated carbon in a multistage countercurrent fluidized bed adsorber. They investigated the process both experimentally and through simulation with various conditions such as different adsorbent feed rate, and gas flow rate. They reported a higher removal efficiency of the VOC in lower gas flow rates, lower initial concentration of VOC, and higher adsorbent feed rate. The experimental data was further used to verify the results from the simulation (Davarpanah, et al., 2020).

Mohanty et.al assessed the adsorption of carbon dioxide (CO_2), both experimentally and mathematically, through a counter current three-staged fluidized bed reactor using hydrated lime particles as the adsorbent. They claimed that the removal efficiency is predominantly affected by adsorbents' flow rate and CO_2 concentration (Mohanty & Meikap, 2011).

The adsorption of VOCs was also investigated on a polymeric adsorbent in a circulating fluidized bed reactor (Song et al., 2005) and heterogeneous alumina-catalyst adsorbents (Dolidovich et al., 1999). Kamravaei et.al studied the multicomponent adsorption of a mixture of nine VOCs in a fixed and a fluidized bed reactor. The results showed 30% less heel build up for the activated carbon in the fluidized bed reactor (Kamravaei, et al., 2017).

Although various cases of adsorption in fluidized beds have been investigated, there needs to be additional research on the nature of competitive adsorption for multicomponent systems. The effect of the chemical/physical properties (polarity, aromaticity, steric hindrance, and boiling point) on competitive adsorption in fluidized beds needs to be studied further individually.

Chapter 3:   Materials and methods

In this chapter materials and methods are discussed. The adsorbents and adsorbates properties as well as adsorption experiments, the multi-staged fluidized bed setup configuration, the relevant calculations, characterization tests, and gas chromatography- Mass Spectrometry (GC-MS) analysis are presented and described.

3.1. Adsorbents

The two adsorbents used in this study are microporous beaded activated carbon (BAC) provided by Kureha Corporation and ZEOCAT F603 (50:50 wt. %) mixture of ZSM-5 & USY provided by ZEOCHEM.

The pore size distribution of the virgin BAC is shown in **Figure 3.1**. As it is observed, the pores are predominantly micropores with the size of less than 20 Å (2 nm). The analysis was carried out using a micropore surface analysis system using nitrogen as the gas (IQ2MP, Quantachrome) (Kamravaei, 2014; Lashaki, et al., 2012).
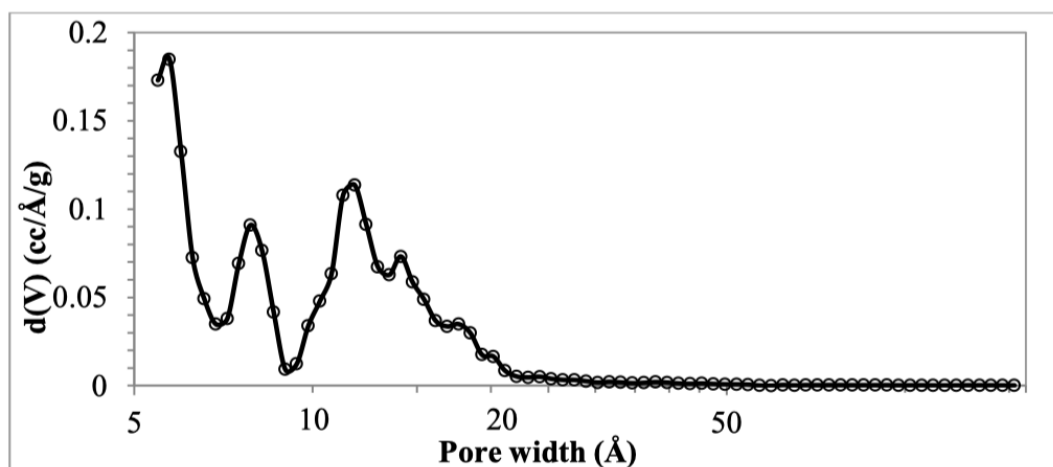
Figure 3.1. Pore size distribution of virgin BAC (adapted from (Kamravaei, 2014)**)**

ZSM-5 and USY were constituents of ZEOCAT F603 which have MFI (Mobil Five) and FAU (Faujasite) framework topologies, respectively. ZSM-5 and USY structures and pore size values are depicted in **Figure 3.2** and , respectively. ZSM-5 is a hydrophobic high-silica zeolite which comprises of 10-membered-ring pores that are marginally elliptical and have dimensions of 5.5×5.1 Å and 5.6×5.3 Å with small cavities. Hydrophilic low-silica USY, on the other hand, has 12-membered-ring pores with slightly larger pores of 7.4×7.4 Å and large cavities. Other aspects of ZSM-5 and USY pore structures are demonstrated in **Figure 3.4** and **Figure 3.5**, respectively (Baerlocher & Olson, 2007; Slawek et al., 2018; Weitkamp, 2000; Xu et al., 1990; Yan, et al., 2003).
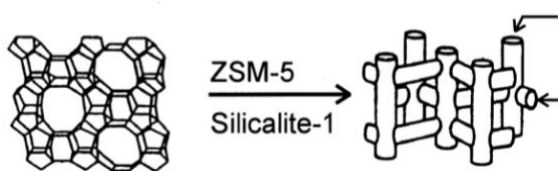
Figure 3.2. Structure and pore size of ZSM-5, the arrows show the entrance of the pores (adapted from (Weitkamp, 2000))
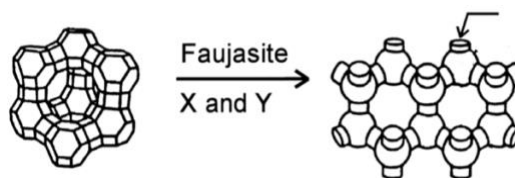
Figure 3.3. Structure and pore size of USY, the arrows show the entrance of the pores (adapted from (Weitkamp, 2000))
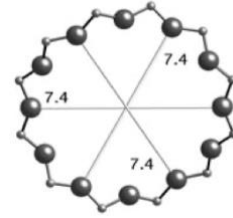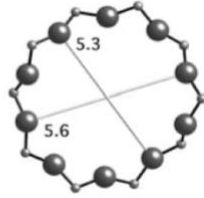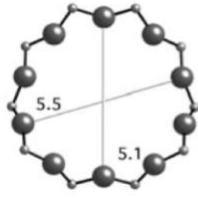
Figure 3.4. Pore shape and size of ZSM-5, values are in Å (adapted from (Baerlocher, L.B., & Olson, 2007))

Figure 3.5. Pore shape and size of USY, values are in Å (adapted from (Baerlocher, L.B., & Olson, 2007))

Table 3.1 represents the properties of the adsorbents. Both adsorbents are beaded shaped and have similar apparent densities. Compared to ZEOCAT F603, Kureha BAC G-70R has a higher surface area, internal porosity, micropore volume, and total pore volume.

Table 3.1. Properties of adsorbents used in this study
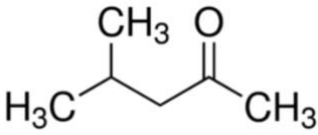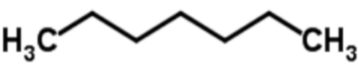
Parameter	Kureha BAC G-70R		ZEOCAT F603	
	Value	Unit	Value	Unit
Mean diameter, d_p	7.5×10^{-4}	m	5×10^{-4}	m
Surface area, A	1349	m² g⁻¹	380	m² g⁻¹
Apparent density, ρ_p	601	kg m⁻³	660	kg m⁻³
Internal porosity, ε_p	0.56	--	0.23	--
Shape factor, ϕ	1	--	1	--
Particle size	0.7	mm	0.5	mm
Shape	Beads	--	Beads	--
Micropore volume	0.49	cm³/g	0.1	cm³/g
Total pore volume	0.57	cm³/g	0.34	cm³/g

3.2. Adsorbates

The VOCs used in this study are typical solvents in the automotive paint industry. Four pairs of chemicals were tested in a binary mixture in order to investigate each effect individually. Each pair of the compounds is listed in separate tables, for the different tests as below. An attempt was made to choose each pair as similar as possible in their properties except for the targeted property.
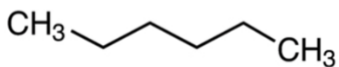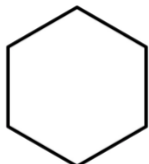
For studying the effect of adsorbate polarity, methyl isobutyl ketone (polar compound) and heptane (n-heptane, non-polar compound) were chosen. Both compounds have similar molecular weight and aromaticity state. Their properties are shown in **Table 3.2**.

Table 3.2. Compounds for polarity effect test

Compound	Parameter	Value	Structure
MIBK	Dipole moment	2.7 D (polar)	
	Molecular weight	100.16 g mol^{-1}	
	Boiling point	116 ℃	
	Structure	Non-aromatic	
Heptane	Dipole moment	0 D (non-polar)	
	Molecular weight	100.21 g mol^{-1}	
	Boiling point	98.42 ℃	
	Structure	Non-aromatic	
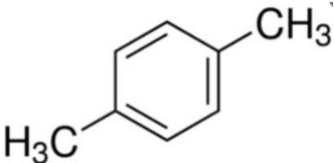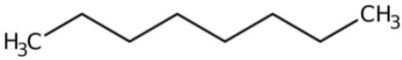
Hexane (n-hexane) and cyclohexane were chosen for investigating the steric hindrance effect. The properties of hexane and cyclohexane are summarized in **Table 3.3**.

Table 3.3. Compounds for steric hindrance effect test

Compound	Parameter	Value	Structure
Hexane	Dipole moment	0.017 D	
	Molecular weight	86.18 g mol^{-1}	
	Boiling point	69 ℃	
	Structure	Non-aromatic	
Cyclohexane	Dipole moment	0 D	
	Molecular weight	84.16 g mol^{-1}	
	Boiling point	80 ℃	
	Structure	Non-aromatic	
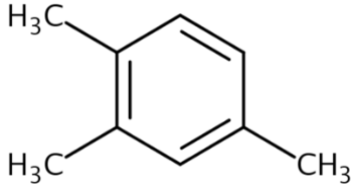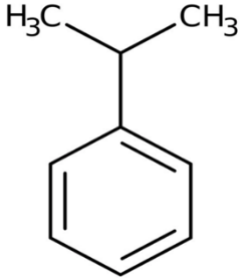
The effect of adsorbate aromaticity on competitive adsorption was tested using p-xylene and octane (n-octane). Their properties are listed in **Table 3.4**. Aromatics are planar and monocyclic systems with (4n+2) π electrons (Clayden et al., 2001).

Table 3.4. Compounds for aromaticity effect test

Compound	Parameter	Value	Structure
P-xylene	Dipole moment	0.081 D	
	Molecular weight	106.16 g mol^{-1}	
	Boiling point	138.4 ℃	
	Structure	Aromatic	
Octane	Dipole moment	0.021 D	
	Molecular weight	114.23 g mol^{-1}	
	Boiling point	125.6 ℃	
	Structure	Non-aromatic	

1,2,4-trimethylbenzene (TMB) and cumene were selected to study the boiling point effect. These isomers share the similar properties except for the boiling point. They are both nonpolar and aromatic. Their properties are shown in **Table 3.5**.

Table 3.5. Compounds for boiling point effect test

Compound	Parameter	Value	Structure
TMB	Dipole moment	0.291 D	
	Molecular weight	120.19 g mol^{-1}	
	Boiling point	170 ℃	
	Structure	Aromatic	
Cumene	Dipole moment	0.79 D	
	Molecular weight	120.19 g mol^{-1}	
	Boiling point	152.4 ℃	
	Structure	Aromatic	

3.3. Adsorption experiment

3.3.1. Isotherm experiments

The setup for the adsorption isotherm is schematically shown in **Figure 3.6**. The adsorber was a fixed bed reactor (a glass reactor with the length of 120 mm and inner diameter of 5mm) and its temperature was measured by a thermocouple (Omega) and controlled via a data acquisition and control system (DAC). This system consisted of LabVIEW program (National Instruments), a software through which the temperature is set. On average, 80 mg of adsorbents was used for each test. The gas used for the isotherm experiments was nitrogen (99.999% purity). The flow rate was adjusted with the mass flow controller and each VOC was injected into the stream through the injection port (wrapped with heating and insulation tape (Omega)), and then sent to the static mixing chamber for obtaining a homogeneous stream. The nitrogen flowrate was set at 0.6 SLPM and the VOC injection rate was set to obtain the target concentration. A photoionization detector (PID, BASELINE VOC-TRAQ II) was used to monitor the effluent concentration and since its maximum acceptable flow rate was 300

ml/min, a diaphragm pump (Thomas, 2002) controlled the flow rate of the stream before entering the PID.
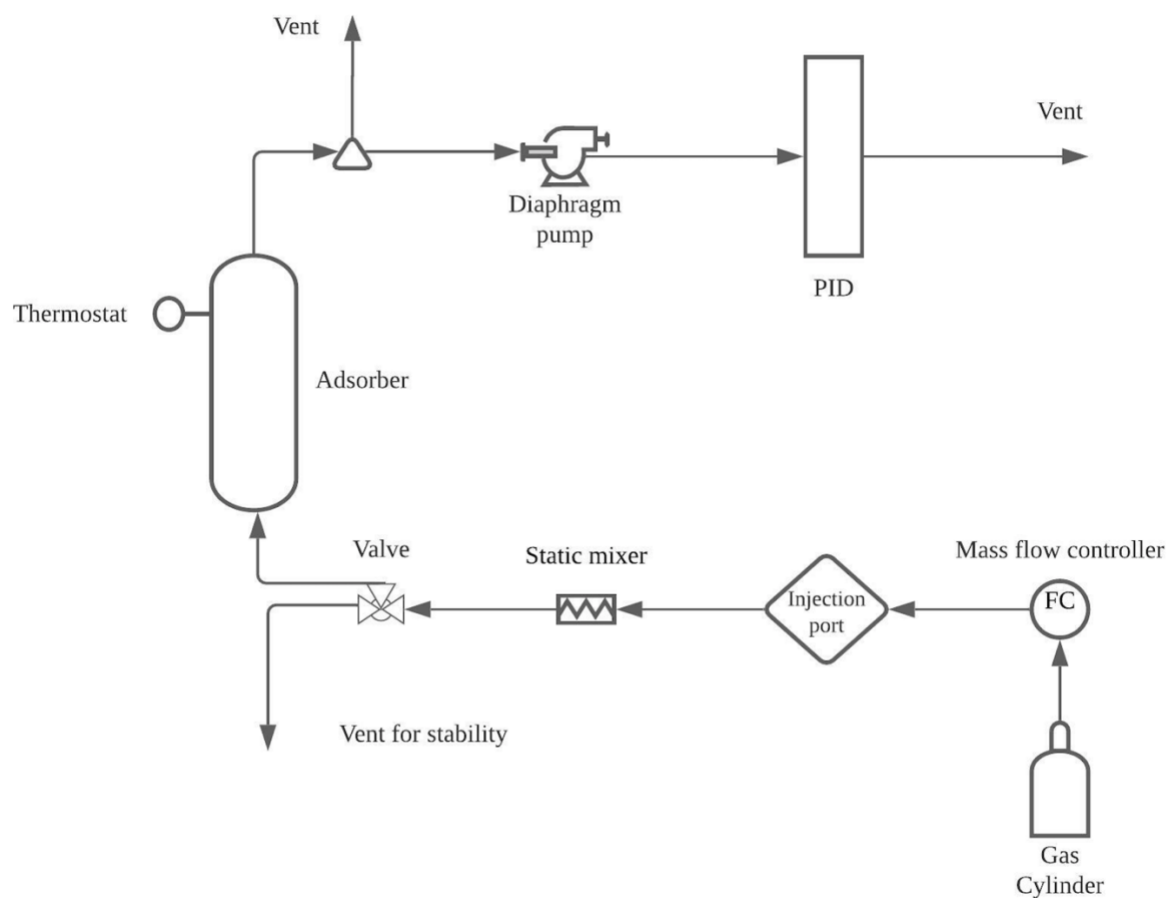
Figure 3.6. The adsorption isotherm setup

To ensure the stability of the inlet concentration, the VOC was injected into the nitrogen stream passing through an empty reactor (no adsorbent) and the time which the effluent concentration became stable was measured. Knowing this time, prior to the isotherm tests, the air was vented before the reactor to reach the desired concentration. To ensure reaching the adsorption equilibrium for the tests, the effluent concentration was monitored until it had the same value of the initial concentration. All the isotherm experiments were duplicated to ensure the accuracy of the data.

For the VOCs with a boiling point of less than 120℃, a gravimetric sorption analyzer (TA instruments, VTI-SA$^+$) was used to carry out the adsorption isotherm test for the relative

pressure ranging from 0.02 to 1. VTI-SA$^+$, a vapor sorption analyzer, is a continuous vapor flow sorption instrument to achieve organic vapor isotherms. This device operates at temperatures ranging from 5 to 150 ℃ at ambient pressure. It contains two chambers for the sample and the reference of which both are exposed to the same temperature. The VOC concentration in the gas stream is determined by the fraction of gas going through the organic solvent evaporator and the fraction of dry gas. Nitrogen (99.999% purity) was the carrier gas in all the experiments. Flow System Software is the program used to control the variables in the isotherm experiments including the adsorption temperature. The results from VTI-SA$^+$ was used to confirm the results obtained from the isotherm setup. This was done through comparing the obtained adsorption capacity from VTI-SA$^+$ and the isotherm setup for the overlapping range of concentration (relative pressure of 0.02 to 0.05).

3.3.2. Multicomponent adsorption

The schematic of the adsorption setup is presented in **Figure 3.7**. The setup consists of a six-stage fluidized bed reactor as the adsorption reactor which is made up of 6 plexiglass cylindrical compartments with the height of 10.4 cm and inner diameter of 7.6 cm. They are separated with perforated trays which would allow the air to pass through the bed but prevent passing of the adsorbents. A protruding downcomer (weir height = 4mm) is placed on each stage to both maintain the amount of adsorbent on each stage and let the adsorbent pass to the stage below (as described in (Davarpanah, 2020)). A calibrated volumetric feeder (Schenck AccuRate) is located on top of the setup controlled by a speed controller. The feeder distributes the adsorbents from the top of the adsorber, the beaded adsorbents are plummeted, and then transported through the stages by gravity. Before adsorption, the adsorbent (Kureha BAC G-70R and ZEOCAT F603) was pre regenerated at 270-288 ℃ to remove any impurities such as

VOCs and moisture from the adsorbents. The adsorbent is then extracted from the adsorbent outlet located at the bottom of the setup.

A desiccant bed (silica gel granules/beads, diameter of 5 mm, Supelco) was used to ensure the dryness of the feed air and a mass flow controller (Alicat Scientific) adjusted the flow rate. The temperature and the humidity of the air were monitored both before entering and exiting the bed. The adsorbate stream (gaseous) was generated via a syringe pump (Chemyx Inc, Nexus 6000) used to inject the desired mixture concentration into the air stream. The concentration of each stage was monitored by a flame-ionization detector (FID, Baseline Mocon, Series 9000). The concentration of each mixture was stabilized before starting the experiment. All the adsorption experiments were duplicated at a temperature of 21℃.

Table 3.6 presents the characteristics of the multicomponent adsorption setup.
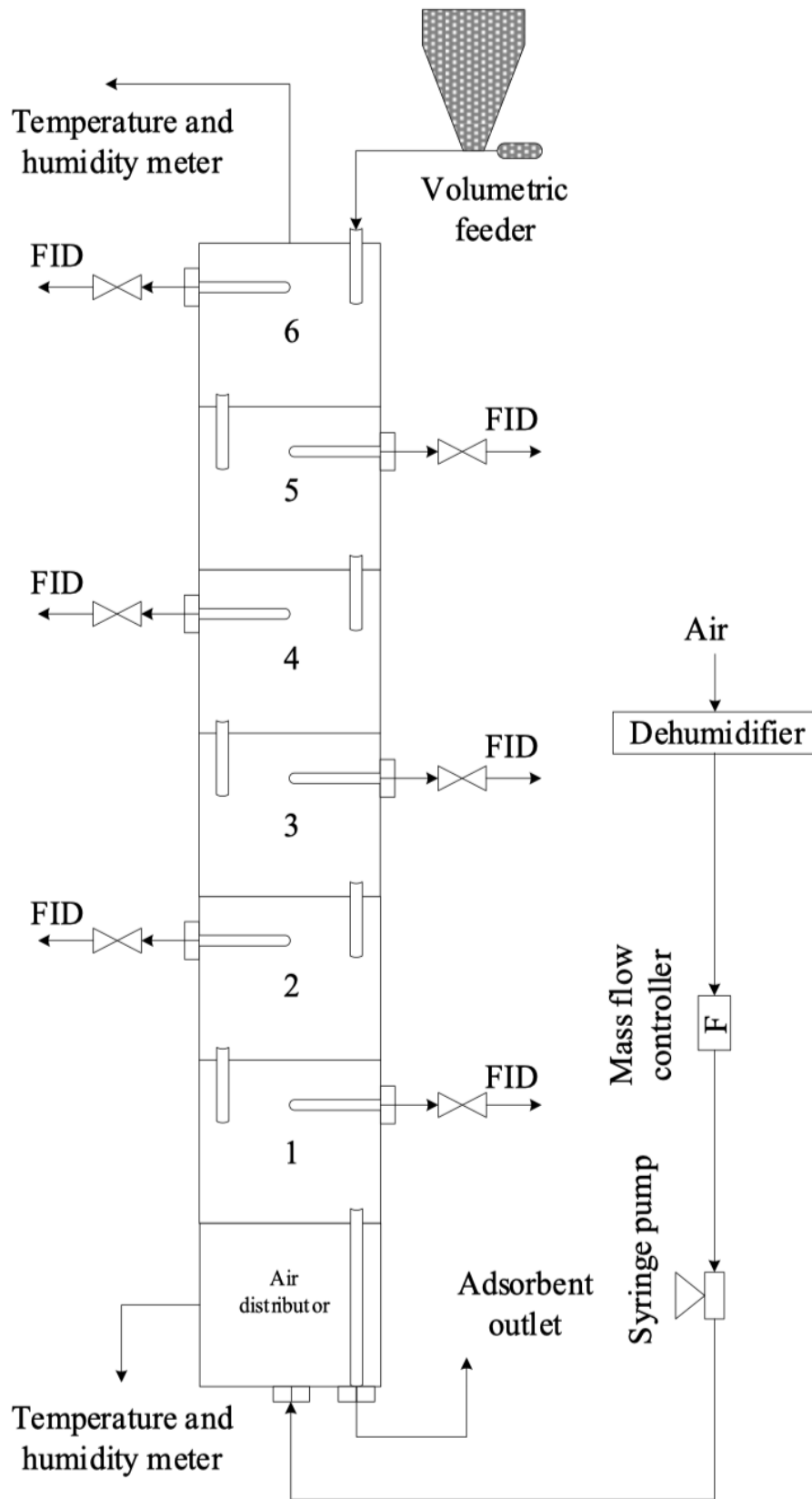
Figure 3.7. The fluidized bed reactor setup

Table 3.6. Adsorption setup characteristics

Parameter	Value	Unit	Reference
Cross section area (Adsorber)	4.56×10^{-3}	m^2	Measured
Temperature	21	℃	Measured
Air density	1.20	kg m^{-3}	(Keenan, Chao, & Kaye, 1992)
Air viscosity	1.82×10^{-5}	kg m^{-1} s^{-1}	(Keenan, Chao, & Kaye, 1992)

The conditions of the experiment are listed in **Table 3.7**. The design of the fluidized bed reactor was done by Shariati (Shariaty, et al., 2015). The feasibility of the conditions is validated by Davarpanah's work (Davarpanah, 2020).

Table 3.7. The conditions of the experiments

Parameter	Value	Unit
Adsorbent feed rate	0.44	g min^{-1}
Airflow rate	250	SLPM
VOC inlet concentration (each compound)	100	ppm
Weir height	4	mm
Temperature	21	℃

The list of the multicomponent experiments is presented in **Table 3.8**. Each effect was investigated using two adsorbents. 100 ppm of each adsorbate was used to make the binary mixtures. The multicomponent tests were duplicated in order to ensure the accuracy of the results.

The calculation of the injection rate is as described in equations **3-1** and **3-2**, assuming ideal gas:

$$\dot{V}\left(\frac{l}{min}\right) = C\ (ppm) * Q\ (SLPM)/10\wedge6 \qquad\qquad \textbf{3-1}$$

$$Injection\ rate\left(\frac{ml}{min}\right) = \dot{V} * P * M/\ R * T * \rho \qquad\qquad \textbf{3-2}$$

Where $\dot{V}$ is volume rate of the VOC, C is the VOC concentration, Q is the air flow rate, P is the pressure, M is the molecular weight of the VOC, R is the universal gas constant, T is the pressure, and ρ is the liquid VOC density.

Table 3.8. List of the multicomponent experiments

Exp. No.	Targeted effect	Adsorbent	Adsorbates	Mixture injection rate (ml/min)
1	Polarity	BAC	MIBK & heptane	0.28
2	Polarity	ZEOCAT F603	MIBK & heptane	0.28
3	Steric hindrance	BAC	Hexane & cyclohexane	0.23
4	Steric hindrance	ZEOCAT F603	Hexane & cyclohexane	0.23
5	Aromaticity	BAC	P-xylene & octane	0.27
6	Aromaticity	ZEOCAT F603	P-xylene & octane	0.27
7	Boiling point	BAC	TMB & cumene	0.29
8	Boiling point	ZEOCAT F603	TMB & cumene	0.29

For each test, a certain amount of time was necessary for the bed to reach a steady state in which the concentration remains the same. The steadiness of the concentration of each stage was checked with the FID.

After reaching the steady state mode, air samples were collected using Tedlar bags (SKC), equipped with polypropylene fittings, for a minute to have an average of the concentration from each stage. The collected samples were analyzed in the same day via the GC-MS device.

3.4. Characterization tests

The characterization of the virgin BAC and ZEOCAT F603 was carried out using nitrogen adsorption (IQ2MP, Quantachrome) at 77 K and the relative pressure ranging from 10^{-6} to 1. First, degassing stage was done prior to the analysis for 30-50 mg of the adsorbent at 120℃ for about 5 hours to eliminate the moisture and organic impurities.

Specific surface area was determined using Brunauer-Emmett-Teller (BET) method and micropore volume was calculated by V-t method. Quenched solid density functional theory (DFT) was used to calculate the pore size distribution and total pore volume.

3.5. X-ray photoelectron spectroscopy (XPS) test

XPS is a quantitative method to measure the elemental composition of an adsorbent's surface and it can determine the binding states of those elements and the detailed chemical bonding. XPS usually investigates to the depth of 10 nm (Guy & Walker, 2016; Mather, 2009). XPS analysis was done on Kureha BAC G-70R in order to detect the chemical bonding and elemental compositions of its surface. In this analysis, the sample is irradiated with X-rays and the kinetic energy of the emitting electrons from the top of the material is measured. The relevant analysis of the result was carried out via CasaXPS software.

3.6. Gas chromatography – mass spectrometry analysis

The concentration of each mixture for every stage of the fluidized bed reactor was measured via a GC-MS system. The system was comprised of a gas chromatograph (Agilent Technologies model 7890A) attached to a mass spectrometer with a Triple-Axis Detector (Agilent Technologies, 5975C). The GC was equipped with a DB-EUPAH capillary column which was 60 m long with a 0.25 mm diameter and 0.25 µm film thickness (Agilent J&W). The injected sample was carried through the column using helium at a flow rate of 0.7 mL/min and a linear velocity of 21.45 cm/s. The injection volume and the injection port temperature were 1 µL and 100 ºC, respectively. The split ratio was 20:1. The NIST/EPA/NIH libraries were used for compound identifications.

Prior to the main analysis, the GC-MS was calibrated with a liquid sample of each binary mixture containing 100 ppm of the selected VOCs. Then, the samples that had been collected from each stage of the reactor were analyzed to obtain the concentration values of each compound in all the stages.

3.7. Experiment calculations

3.7.1. Fluidization calculations

In order to determine the gas velocity/flow rate, one needs to calculate the minimum fluidization velocity (U_{mf}) and minimum fluidization porosity (ε_{mf}) (bed voidage at minimum fluidization). The two parameters are calculated as below in equations **3-3** and **3-4** (Davarpanah et al., 2020):

$$\frac{1.75}{\phi\varepsilon_{mf}^3}Re_{mf}^2 + \frac{150(1-\varepsilon_{mf})}{\phi^2\varepsilon_{mf}^3}Re_{mf} - Ar = 0 \qquad \textbf{3-3}$$

$$Re_{mf} = \frac{\rho_g d_p \boldsymbol{u_{mf}}}{\mu_g}$$

$$Ar = \frac{\rho_g(\rho_p - \rho_g)gd_p^3}{\mu_g^2}$$

$$\boldsymbol{\varepsilon_{mf}} = \frac{1}{6}(6 - \pi) \qquad\qquad \textbf{3-4}$$

All the parameters in the equations **3-1 and 3-2** are described in **Table 3.9**.

Table 3.9. Parameters in 3-3 and 3-4 equations (Davarpanah, 2020)

Description	Symbol
Adsorbent shape factor	ϕ
Reynold's number at u_{mf}	Re_{mf}
Archimedes number	Ar
Gas (air) density	ρ_g
Adsorbent mean diameter	d_p
Gas (air) viscosity	μ_g
Adsorbent density	ρ_p

Both adsorbents were assumed to be spherical. The calculations are partly based on the adsorbents' properties which have been demonstrated before in **Table 3.1**. Other relevant parameters' values are shown in **Table 3.6**.

The minimum fluidization velocity for BAC and ZEOCAT F603 was calculated to be 0.198 and 0.109 m/s, and the minimum required air flow rate to fluidize the bed was 54.29 and 29.87 SLPM, respectively. The air flow rate of 250 SLPM was selected for the experiments which is approximately 5 times the minimum fluidization velocity for BAC and around 8 times the amount for the zeolite as it is the common value in the industry. At the same time, lower

air flow rate enhances the adsorbate removal and 250 SLPM was chosen as the optimal flow rate (Roy et al., 2009).

3.7.2. Adsorption calculations

The adsorption capacity of the adsorbent for the fluidized bed reactor tests is calculated as shown in equations 3-5 and 3-6:

$$Adsorbed\ amount\ \left(\frac{g}{min}\right) = Injection\ rate\ \left(\frac{ml}{min}\right) \times removal\ efficiency \times density\ \left(\frac{g}{ml}\right) \qquad \textbf{3-5}$$

$$Adsorption\ capacity = adsorbed\ amount\ \left(\frac{g}{min}\right) / adsorbent\ feedrate\ \left(\frac{g}{min}\right) \qquad \textbf{3-6}$$

Chapter 4:   Results and discussion

The adsorption isotherms of VOCs are first presented in this section. The tests were done within the concentration range of 50 to 1000 ppm using both Kureha BAC G-70R and ZEOCAT F603.

The effects of polarity, steric hindrance, aromaticity, and the boiling point were investigated on competitive adsorption in a six-stage countercurrent fluidized bed reactor using Kureha BAC G-70R and ZEOCAT F603 as the adsorbents. To find a more reliable correlation between each effect and the competitive adsorption, an attempt was made so that the VOCs in the binary mixtures were as similar as possible in their properties except for the target property. For example, for the polarity effect test, MIBK and heptane were selected, and they are almost identical in their properties except for their polarity. Further, the affinity of the adsorbents for the VOCs was investigated via single-component adsorption through experimentally obtaining the adsorption isotherm.

The results are reported and discussed in terms of the outlet concentration of each stage, removal efficiency, and comparing the adsorption capacity of the VOCs in the multicomponent adsorption test to their equilibrium adsorption capacity at the concentration of 100 ppm. The results and the interpretation of the XPS test as well as the isotherm graphs of each VOC are reported.

4.1. Adsorption isotherm tests

The single-component adsorption isotherm tests were carried out in a fixed bed reactor for all the selected compounds using Kureha BAC G-70R and ZEOCAT F603 and the results are presented in **Figure 4.1**. The results from isotherm tests served two purposes for this research. The first goal was to compare the adsorption capacity of the selected VOCs within the range of 50 to 1000 ppm using Kureha BAC G-70R and ZEOCAT F603. The second goal

was to evaluate the impact of competitive adsorption in the fluidized bed via comparing the equilibrium adsorption capacity of the VOCs at 100 ppm with their adsorption capacity in the multicomponent test.

Compared to its counterpart ZEOCAT F603, a higher adsorption capacity for Kureha BAC G-70R is observed, due to its higher surface area and pore volume (both total and micropore). Further, among the VOCs, the Kureha BAC G-70R showed the highest adsorption capacity for TMB in the entire concentration range, while hexane and octane had the lowest adsorption capacity. A notable change in the adsorption capacity of MIBK and p-xylene was observed at concentration higher than 100 ppm. In the low concentration region (< 100 ppm), the adsorbed amount of hexane, cyclohexane, p-xylene and octane are relatively similar.

Regarding the zeolite, all the VOCs approximately showed similar adsorption capacity except for cyclohexane, which might be due to the cyclohexane molecular structure and conformations. In the range of less than 100 ppm, MIBK and heptane had the highest adsorption capacity. At concentrations higher than100 ppm, a considerable change in p-xylene, TMB, and cumene adsorption capacity is observed.

In addition, the required amount to reach the maximum capacity was higher for Kureha BAC G-70R. This can be attributed to the higher surface area and pore volume of BAC as well as its hierarchal pore structure (Li, et al., 2020).
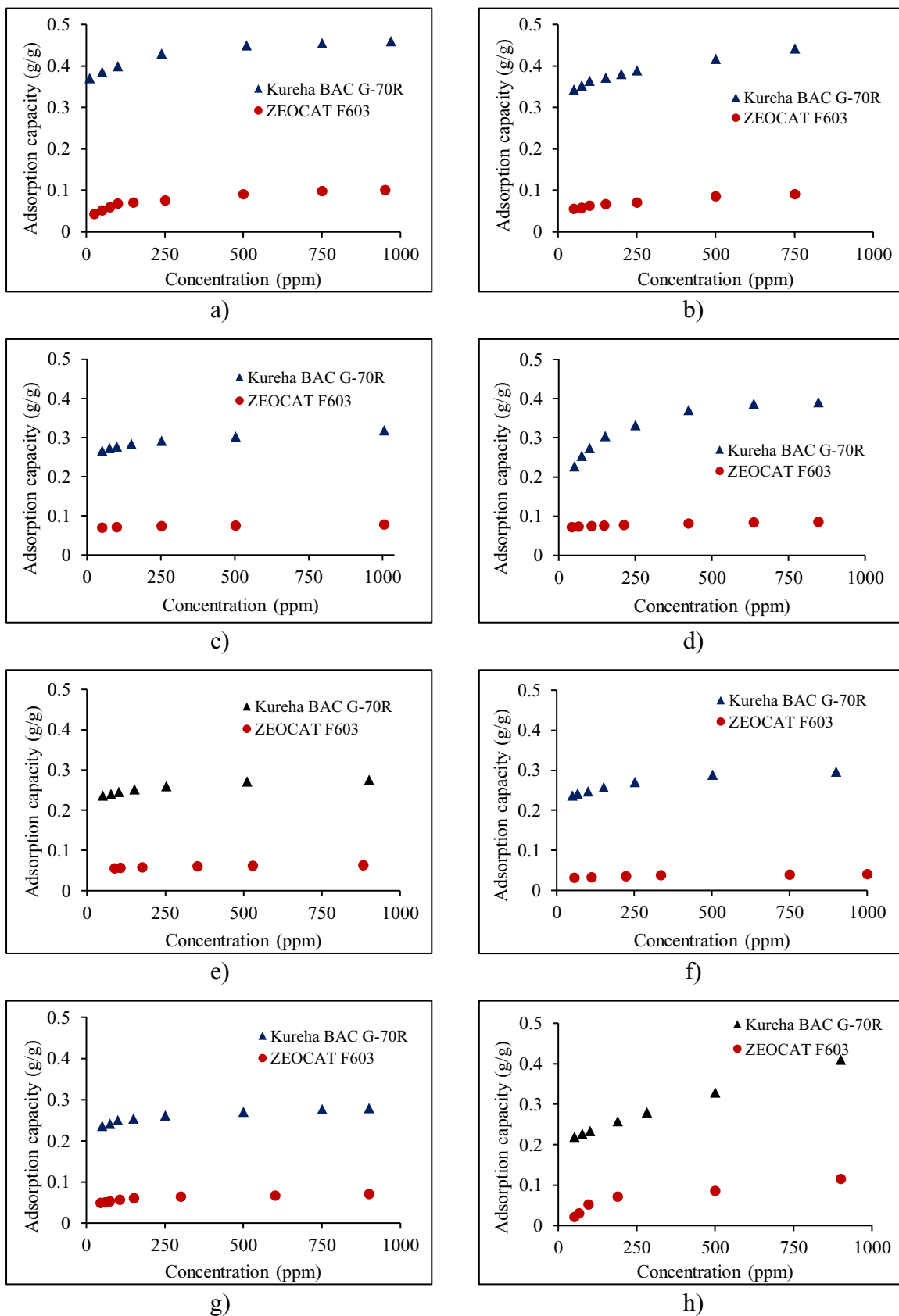
Figure 4.1. VOC adsorption isotherms on Kureha BAC G-70R and ZEOCATE F603 a) TMB, b) cumene, c) heptane, d) MIBK, e) hexane, f) cyclohexane, g) octane, and h) p-xylene

4.2. Effect of polarity

As discussed before, the impact of the polarity of the adsorbate on adsorption is dependent on the activated carbon hydrophilic sites, and zeolites show a tendency toward polar compounds because of their local electrostatic forces in their framework.

To study the effect of polarity, MIBK (a polar compound), and heptane (a non-polar compound) were chosen as the adsorbates. MIBK and heptane have non-aromatic structures, similar molar mass values and boiling points. The assumption was that the multicomponent test using MIBK and heptane would generate a more reliable correlation between the adsorbates' polarity and the affinity of the activated carbon toward polar compounds. The properties of these VOCs are listed in **Table 3.2**. A binary mixture composed of 100 ppm of each VOC was made for the experiment. The results of the experiments using Kureha BAC G-70R and ZEOCAT F603 are as follows.

4.2.1. Kureha BAC G-70R test

The outlet concentration and the removal efficiency from each stage of the fluidized bed reactor using Kureha BAC G-70R are shown in **Figure 4.2**. The outlet concentration for both compounds were similar in all stages and the removal efficiency of both compounds was 95 to 96%. Based on the results, a similar amount of adsorption was obtained for both components in all the stages which shows that, at the tested concentrations, BAC did not show a greater affinity toward the polar compound.

As shown in **Figure 4.3**, the adsorption capacity values of the compounds in the multicomponent test were 6 to 7% less than of the equilibrium adsorption capacity values at 100 ppm. The equilibrium adsorption capacity for both VOCs on BAC was the same which indicates that this adsorbent had a similar affinity toward both compounds at the concentration of 100 ppm.

In this research, MIBK and heptane were the selected VOCs which have non-aromatic structures, similar molar mass values and close boiling points. The assumption was that the multicomponent test using MIBK and heptane would generate a more reliable correlation between the adsorbates' polarity and the affinity of the activated carbon toward polar compounds.

Reinoso et. al. reported that the amount of oxygen surface groups on the surface of the microporous activated carbon is of tremendous importance in adsorption of polar molecules (Rodriguez-Reinoso et al., 1992). Meng et. al. stated that the oxygen-containing groups on the surface of activated carbons facilitate the adsorption of polar VOCs (Meng et al., 2019). A polar adsorbate would prefer to initially occupy the polar sites on activated carbon (Fletcher et al., 2006). The results from the XPS analysis demonstrated the existence of oxygen-containing groups on BAC surface (further explained in subsection 4.6). Since a similar adsorption capacity was observed for both of the polar and non-polar component, it is assumed that the hydrophilic sites (oxygen-containing groups) on BAC surface were not sufficient to affect the adsorption of the polar adsorbate. BAC surface showed a similar attraction for both of the polar and non-polar compound.

Figure 4.2. Effect of adsorbate polarity on the stage-wise outlet concentration and removal efficiency using Kureha BAC G-70R where 0 is the inlet, 1 is the bottom stage, and 6 is the top stage of the fluidized bed (the error bars indicate the standard deviation of two tests)

Figure 4.3. Comparison of the adsorption capacity at 100 ppm of heptane and MIBK on Kureha BAC G-70R from the multicomponent test (the fluidized bed test) and the single component test (the error bars indicate the standard deviation of two tests)

4.2.2. ZEOCAT F603 test

As seen in **Figure 4.4**, the outlet concentration for both heptane and MIBK were similar until stage 3, but from that stage on, a higher adsorption of MIBK took place. The overall removal efficiency of MIBK was 20% higher than of heptane which indicates the tendency of ZEOCAT F603 toward the adsorption of the polar compound in case of competitive adsorption.

Figure 4.5 depicts that both compounds have similar single-component equilibrium adsorption capacity of 7-7.5%. However, the adsorption capacity of heptane in the multicomponent test was lower by 4% compared to that of MIBK. The lower removal efficiency of heptane can be attributed to competitive adsorption between the VOCs.

Calleja et. al. investigated the multicomponent adsorption of multiple compounds with ZSM-5 zeolite and a higher adsorption of polar molecules on the zeolite with a lower Si/Al ratio was reported. A decrease in Si/Al ratio was claimed to increase surface heterogeneity and electrostatic field inside zeolite pores (Calleja et al., 1998). The observed affinity of ZEOCAT F603 for the polar compound is assumed to be based on the local electrostatic forces in its framework as well as its low Si/Al ratio, since 50% of this zeolite consists of low-silica USY. Amdebrhan also investigated the effect of polarity of ZEOCAT F603 used in his study. He carried out the adsorption of TMB both from a humid and dry stream and reported a noticeable effect of moisture on TMB adsorption. The uptake of TMB through ZEOCAT F603 decreased in the presence of water, which is a polar compound. The reported affinity of ZEOCAT F603 for polar compounds is consistent with the results of this multicomponent test (Amdebrhan, 2018).
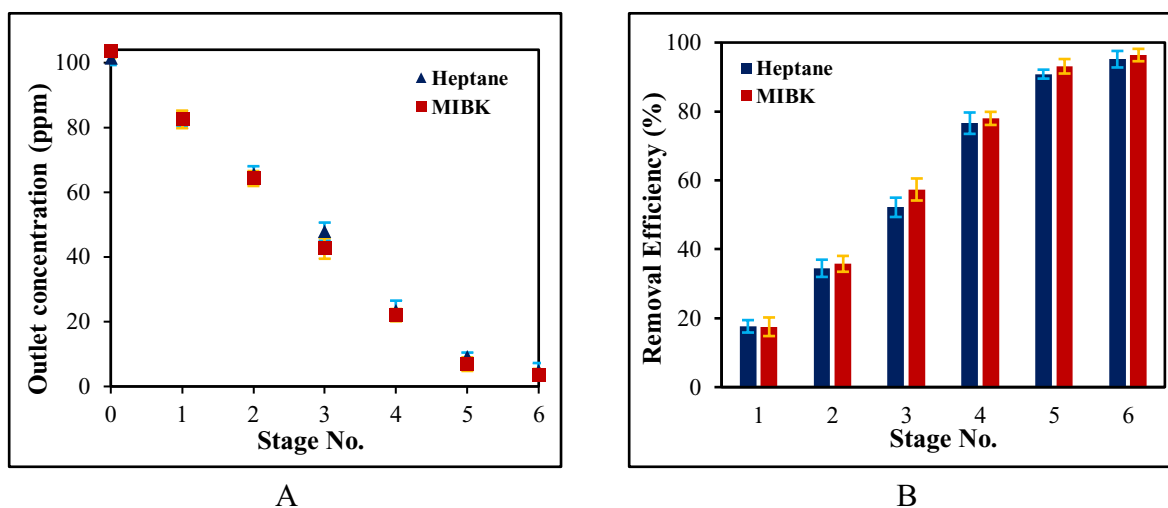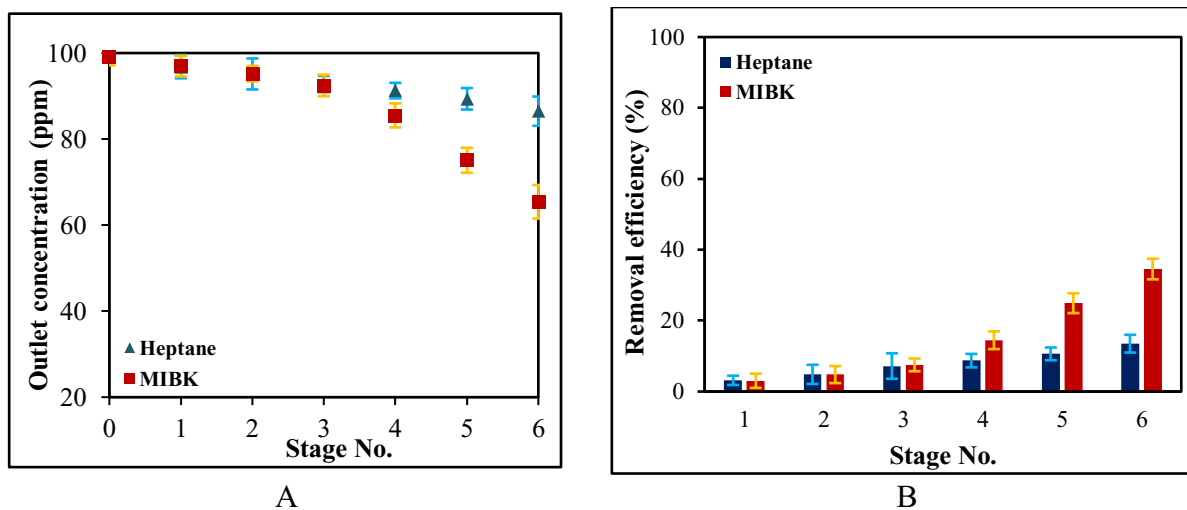
Figure 4.4. Effect of adsorbate polarity on the stage-wise outlet concentration and removal efficiency using ZEOCAT F603 where 0 is the inlet, 1 is the bottom stage, and 6 is the top stage of the fluidized bed (the error bars indicate the standard deviation of two tests)

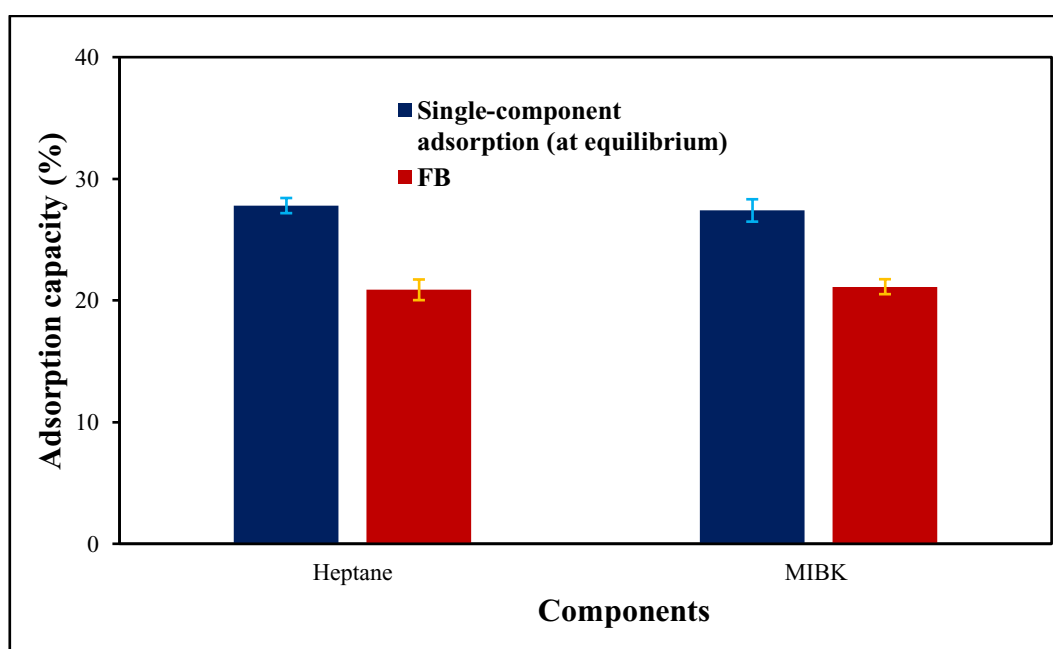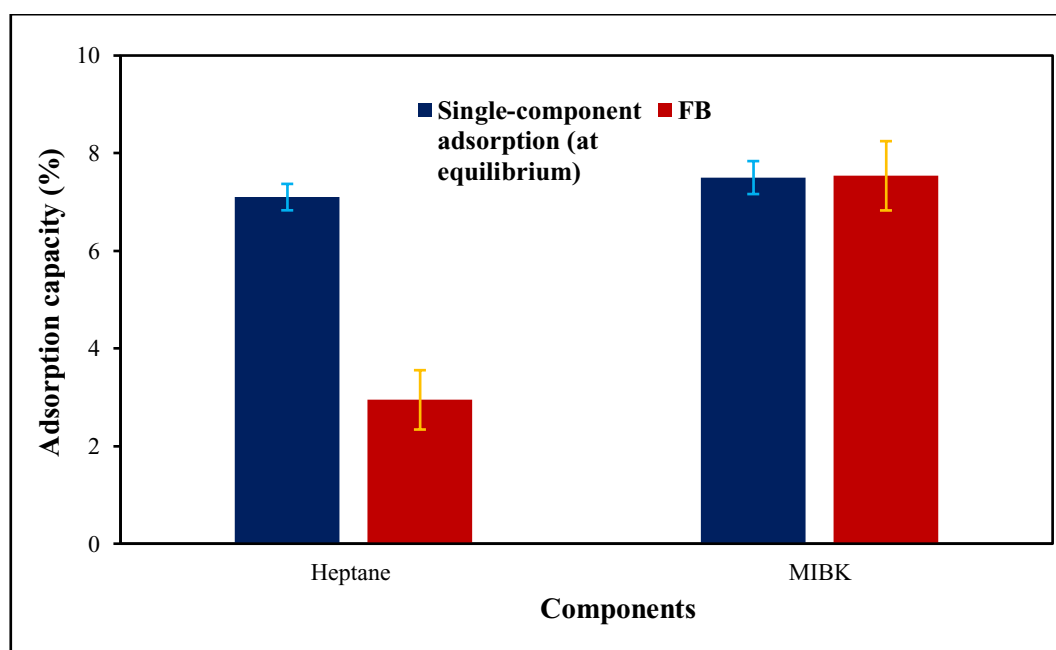

Figure 4.5. Comparison of the adsorption capacity at 100 ppm of heptane and MIBK on ZEOCAT F603 from the multicomponent test (the fluidized bed test) and the single component test (the error bars indicate the standard deviation of two tests)

4.3. Effect of steric hindrance

Steric effects are related to the size and shape of groups existing in the molecule. Not only do these effects have an impact on reaction rates, but also, they drastically change the mechanisms of molecules reaction (Clayden, Greeves, & Warren, 2001).

The critical dimensions of the adsorbate can impact the adsorption process. **Table 4.1** encloses the critical dimensions of hexane and cyclohexane molecules along the x, y, and z symmetry axes of the molecule. The MIN-1 and MIN-2 values are the two smallest minimum dimensions of each molecule. The shape of the adsorbent's pores determines the dimension which is critical for the molecule to enter the pore. For instance, if the pore shape is cylindrical, both MIN-1 and MIN-2 values of the molecules are crucial in their adsorption. But if the pore is slit-shaped, then the only important value is MIN-1 (Webster et al., 1998). Another parameter of adsorbate molecules that is effective on steric separation is the kinetic diameter. In this case, hexane and cyclohexane have the kinetic diameter of 4.3 and 6-6.2 Å, respectively (Li, et al., 2009).

Table 4.1. Molecular x, y, z, MIN-1, and MIN-2 dimensions[1] (the units are in Å)

Compound	X	Y	Z	MIN-1	MIN-2
Hexane	10.344	4.536	4.014	4.014	4.536
Cyclohexane	7.168	6.580	4.982	4.982	6.580

The shape of VOCs has a high impact on adsorption (Li et al., 2009; Li, et al., 2020). According to Cavalcante et al, the diffusion of cyclic compounds is highly affected by steric hindrance, and the adsorption process of these compounds is dependent on how their molecules can fit the pores of the adsorbent (Cavalcante & Ruthven, 1995). It is widely known that the

---

[1] Values were retrieved from (Webster, Drago, & Zerner, 1998)

adsorption of linear alkanes on most microporous materials is favorable compared to the branched isomers (Bozbiyik, et al., 2014).

Aside from the difference in their dimensions, hexane and cyclohexane are different in terms of their structure. Hexane is a saturated acyclic/linear alkane while cyclohexane is a saturated hydrocarbon and has a cyclic non-planar structure with six-membered rings. Not all the carbon atoms in its structure are in the same plane and the bond angles are 109.5°. Cyclohexane can have various types of conformations. The first one is called the chair conformation since there are 4 carbon atoms in the same plane and the other two atoms are above and below it, respectively. A simplified models is shown in **Figure 4.6** (Clayden et al., 2001).

Another type is known as the boat conformations in which 4 carbon atoms are in the same plane but the other two are placed above. This conformation, however, is not a stable one. The model is demonstrated in **Figure 4.7** (Clayden et al., 2001).
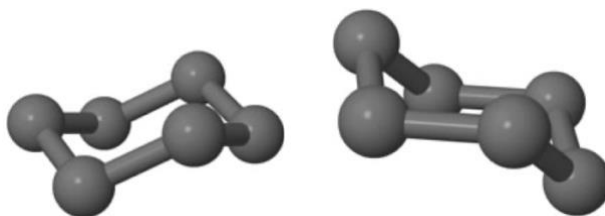
Figure 4.6. The chair conformation of cyclohexane (adapted from (Clayden et. al., 2001))
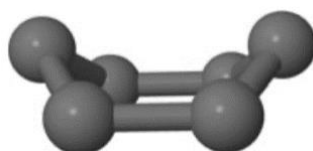
Figure 4.7. The boat conformation of cyclohexane (adapted from (Clayden et al., 2001))

It was assumed that the steric hindrance effect would impact the adsorption of cyclohexane due to its larger molecule, cyclic non-planar structure, and various conformations. The results obtained from the multicomponent adsorption on Kureha BAC G-70R and ZEOCAT F603 are as follows.

4.3.1. Kureha BAC G-70R

The results from the multicomponent test are shown in **Figure 4.8**. The removal efficiency of both VOCs is close in stage 1, but in stages 2, 3, and 4, the displacement of cyclohexane by hexane can be observed since the concentration in those stages are higher than the first stage. Eventually, the overall removal efficiency of cyclohexane was lower than that of hexane by about 30%.

The single-component adsorption test was also done for hexane and cyclohexane. Although they have similar equilibrium adsorption capacity, they are different in terms of their adsorption capacity in the multicomponent test by 6%, as demonstrated in **Figure 4.9**. This can represent the impact of competitive adsorption in the multicomponent test.

For activated carbons to evade the steric hindrance effects (have a higher removal efficiency), the adsorbate molecules have to be small enough (Nevskaia et al., 2004). Among the VOCs, cyclohexane has a cyclic structure and larger critical molecular dimensions. In contrast, hexane has a linear structure and as stated earlier, microporous solids show tendency toward saturated hydrocarbons with linear structures. Since BAC G-70R is highly microporous, it can be presumed that the steric hindrance effect was the inhibiting factor for the adsorption of cyclohexane, while the linearity of hexane facilitated its adsorption. Not only did hexane achieve a higher overall removal efficiency, but also it displaced its counterpart in the middle stages of the fluidized bed.
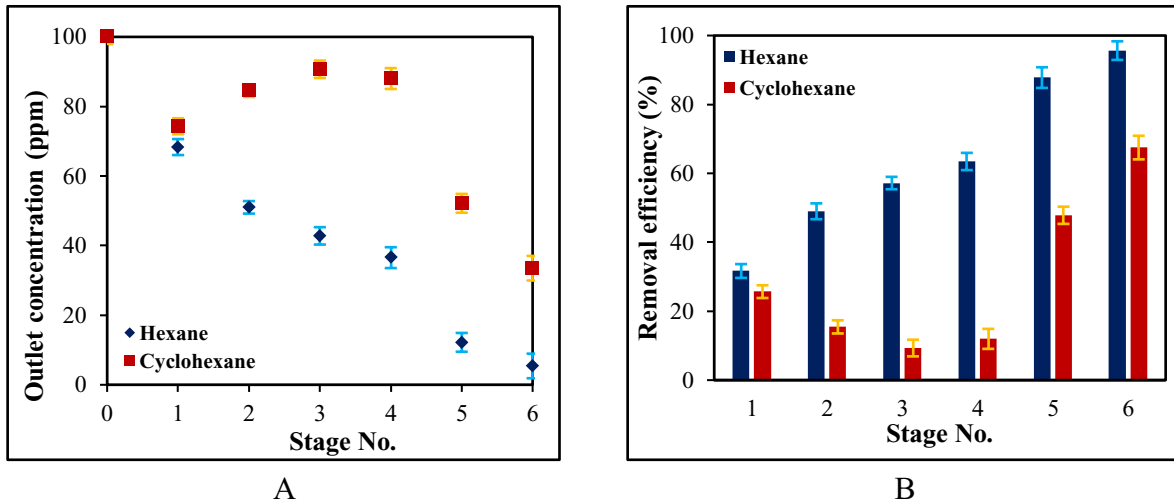
Figure 4.8. Effect of steric hindrance on the stage-wise outlet concentration and removal efficiency using Kureha BAC G-70R where 0 is the inlet, 1 is the bottom stage, and 6 is the top stage of the fluidized bed (the error bars indicate the standard deviation of two tests)

Figure 4.9. Comparison of the adsorption capacity at 100 ppm of hexane and cyclohexane on Kureha BAC G-70R from the multicomponent test (the fluidized bed test) and the single component test (the error bars indicate the standard deviation of two tests)

4.3.2. ZEOCAT F603

The results in **Figure 4.10** show that hexane had a removal efficiency of around 25% in the multicomponent test while the adsorption of cyclohexane was completely inhibited. Cyclohexane was displaced by hexane in the competitive adsorption in all stages of the fluidized bed reactor. **Figure 4.11** demonstrates the fluidized bed reactor's adsorption capacity and the equilibrium adsorption capacity for hexane and cyclohexane at 100 ppm. Cyclohexane's equilibrium adsorption capacity was lower than that of hexane by approximately 50% and ZEOCAT F603 was more favorable toward hexane adsorption.

As mentioned earlier, ZEOCAT F603 consists of ZSM-5 and USY (50:50 wt.%). These two zeolites are different in terms of their pore size as shown in **Figure 3.4** and **Figure 3.5**. ZSM-5 possesses a MFI framework with small cavities and almost cylindrical pores. USY too has cylindrical pores but with a FAU framework containing large cavities. Since both zeolites' pores are almost cylindrical, it is assumed that both MIN-1 and MIN-2 values of the hexane and cyclohexane molecules were essential in the adsorption of these VOCs.

According to previous studies, the existing channels and cavities in the zeolites' framework enable them to show selective adsorption. Additionally, the linearity of saturated hydrocarbons facilitates their adsorption process in microporous adsorbents (Bozbiyik, et al., 2014; Shwanke et al., 2012; Slawek et al., 2018). Further, the study of Slawek et. al. on the adsorption of cyclohexane in various zeolites presented the effect of cyclohexane conformation on its diffusion and placement into the zeolites' pores. Zeolites with the MFI framework were claimed to be selective toward the t-boat conformation while zeolites with the FAU framework do not differentiate between the conformations of cyclohexane. This phenomenon was attributed to the size and shape of the zeolites' channels and cavities (Slawek et al., 2018). A superior interaction of n-alkanes throughout the small pores of ZSM-5 with a MFI framework

compared to zeolite Y with a FAU framework was reported by Denayer et. al (Denayer et al., 1998).

Thereby, it can be deduced that the adsorption of cyclohexane was hindered due to the framework of ZEOCAT F603, the size and shape of its pores, and cyclohexane molecular properties. This steric hindrance was observed both in cyclohexane's equilibrium and the fluidized bed adsorption capacity. Not only did cyclohexane show a lower equilibrium adsorption capacity compared to hexane, but also its adsorption on the zeolite was completely restrained by hexane in the competitive adsorption. Further, based on Denayer et al. study, since hexane is a part of n-alkanes family, it is assumed that most of its uptake occurred via ZSM-5 rather than USY.

A   B
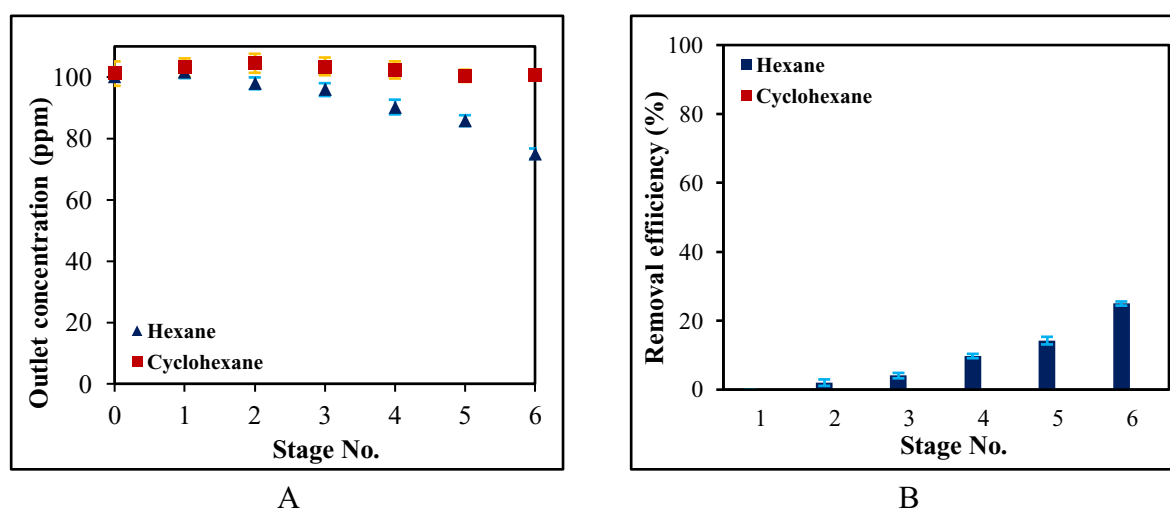
Figure 4.10. Effect of steric hindrance on the stage-wise outlet concentration and removal efficiency using ZEOCAT F603 where 0 is the inlet, 1 is the bottom stage, and 6 is the top stage of the fluidized bed (the error bars indicate the standard deviation of two tests)
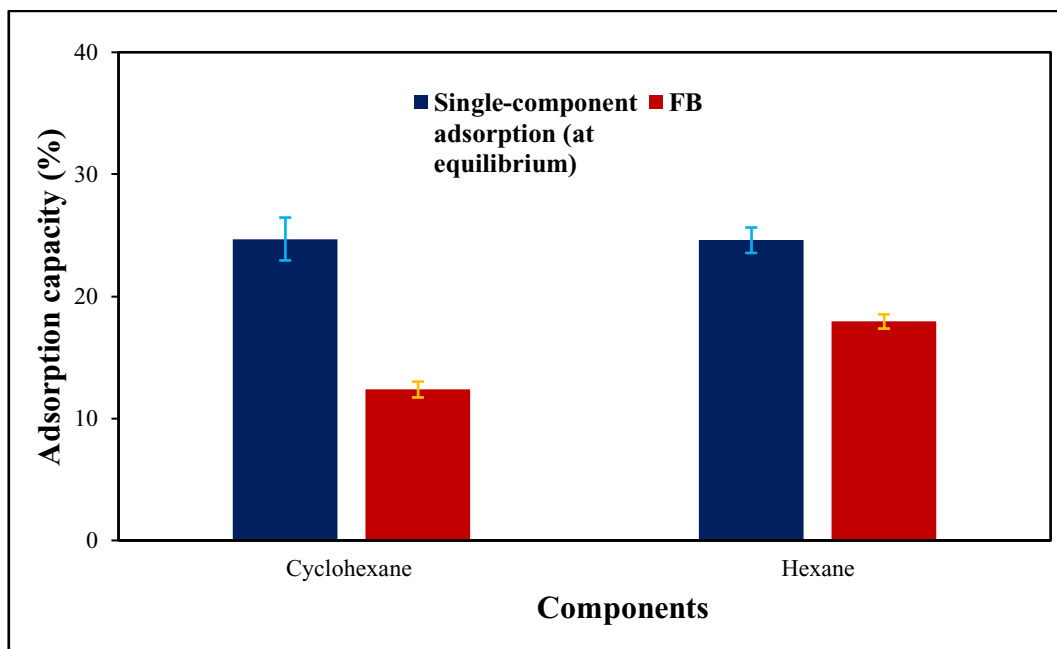
Figure 4.11. Comparison of the adsorption capacity at 100 ppm of hexane and cyclohexane on ZEOCAT F603 from the multicomponent test (the fluidized bed test) and the single component test (the error bars indicate the standard deviation of two tests)

4.4. Effect of aromaticity

Earlier in this study, the mechanisms with which aromatic compounds are adsorbed on the surface of activated carbons and zeolites were discussed. To evaluate the effect of aromaticity on competitive adsorption in the fluidized bed reactor, p-xylene and octane were chosen. As specified in **Table 3.4**, p-xylene possesses an aromatic, and planar structure while octane is a linear saturated hydrocarbon. Both VOCs are non-polar and have similar molar mass and boiling point. The results of the multicomponent test in the fluidized bed reactor using Kureha BAC G-70R and ZEOCAT F603 are reported in the following subsections.

4.4.1. Kureha BAC G-70R test

Figure 4.12 presents the outlet concentration and the removal efficiency from each stage of the fluidized bed reactor, respectively. Throughout the stages 2, 3, & 4 of the reactor, it is observed that p-xylene showed a higher removal efficiency than did octane.

The comparison of the equilibrium adsorption capacity and the fluidized bed reactor test adsorption capacity is presented in **Figure 4.13**. The obtained adsorption capacity for p-xylene and octane from the fluidized bed reactor was similar to their adsorption at equilibrium state which shows the high efficiency of the fluidized bed regarding the adsorption of these VOCs.

Higher adsorption of the aromatic component, p-xylene, was observed in the middle stages (2, 3, &4). BAC became more saturated as it moved to the lower stages, and as a result, less adsorption sites were available on its surface. The fresher BAC in stages 5 and 6 seemed to have a sufficient capacity to achieve a similar removal efficiency for the VOCs, but after being partially saturated, BAC had a higher adsorption capacity for p-xylene by 10% for stages 2 and 4, and 15% for stage 3. This affinity for the aromatic compound can be ascribed to π-π interaction on BAC surface. This interaction is attributed to the C=C bond on BAC surface which may indicate the presence of graphitic carbon. The observed affinity can also be ascribed to the non-polar surface attributes of BAC (Wang et al., 2004). Additional information about BAC surface using the interpretation of X-ray photoelectron spectroscopy (XPS) test and BAC affinity toward the aromatics is available in Section 4.6.

Figure 4.12. Effect of adsorbate aromaticity on the stage-wise outlet concentration and removal efficiency using Kureha BAC G-70R where 0 is the inlet, 1 is the bottom stage, and 6 is the top stage of the fluidized bed (the error bars indicate the standard deviation of two tests)
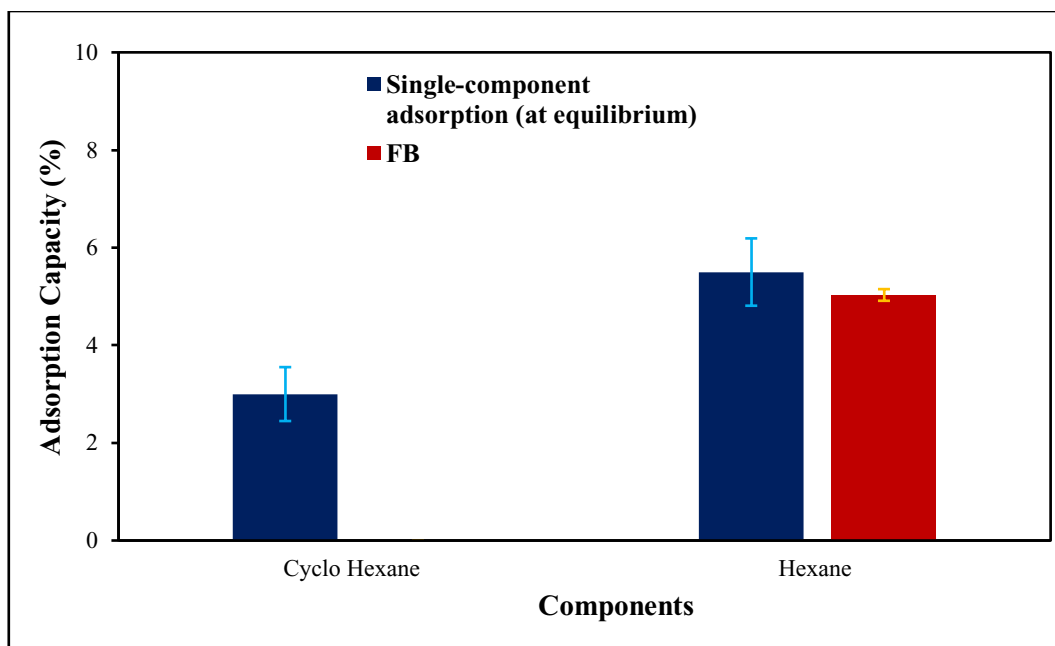

Figure 4.13. Comparison of the adsorption capacity at 100 ppm of octane and P-xylene on Kureha BAC G-70R from the multicomponent test (the fluidized bed test) and the single component test (the error bars indicate the standard deviation of two tests)

4.4.2. ZEOCAT F603 test

Figure 4.14 presents the outlet concentration and the removal efficiency of each stage of the fluidized bed from the multicomponent test using ZEOCAT F603. It is observed that the adsorption behavior of p-xylene and octane onto the zeolite was similar. The results suggest that ZEOCAT F603 is not favorable toward the adsorption of aromatic compounds.

P-xylene and octane also showed a similar equilibrium adsorption capacity at 100 ppm. As shown in **Figure 4.15**, both VOCs had the adsorption capacity of 5.4%. Based on p-xylene and octane showing similar adsorption capacity, it is presumed that the zeolite framework and surface characteristics did not cause this adsorbent to have a higher tendency toward aromatics.

The surface of ZEOCAT F603 does not have similar features to BAC. As discussed earlier, the graphitic carbon on the surface may have caused a higher adsorption capacity for p-xylene through (π-EDA) interactions. The zeolite's surface, however, could not facilitate the adsorption of the aromatic compound in the competitive adsorption.

The cyclic structure of the p-xylene was not influential on its adsorption. Unlike cyclohexane, p-xylene has a planar structure, and it achieved the same amount of adsorption as octane, which has a linear structure. Also, ZEOCAT F603 is a polar adsorbent, and it is assumed that the adsorption of p-xylene took place through the polarity-induced phenomenon (Wang et al., 2004).

In addition, ZEOCAT F603 has lower surface area and pore volume values than the Kureha BAC. Hence its overall removal efficiency for p-xylene and octane was remarkably lower compared to BAC by approximately 70%.
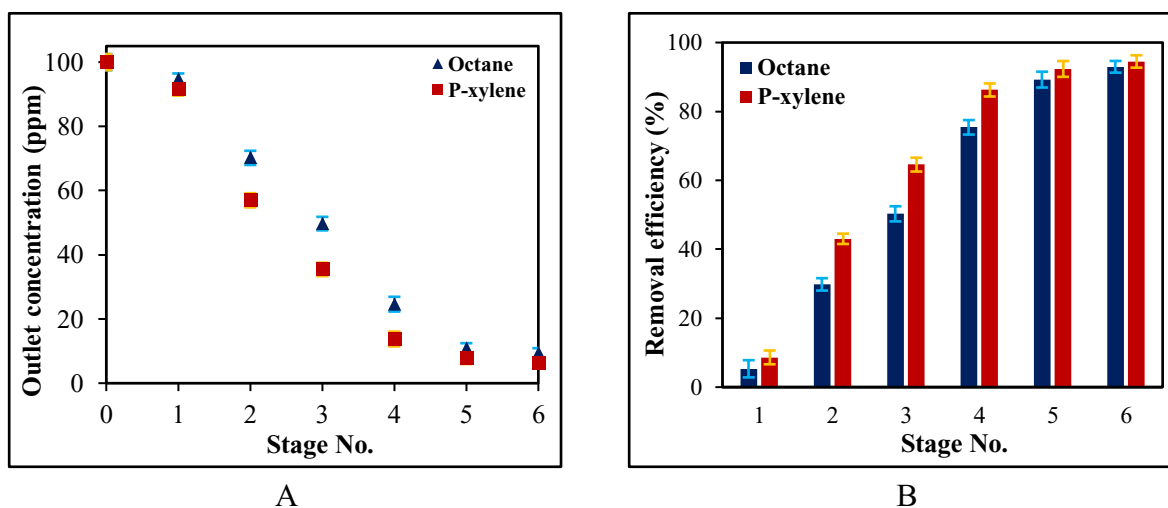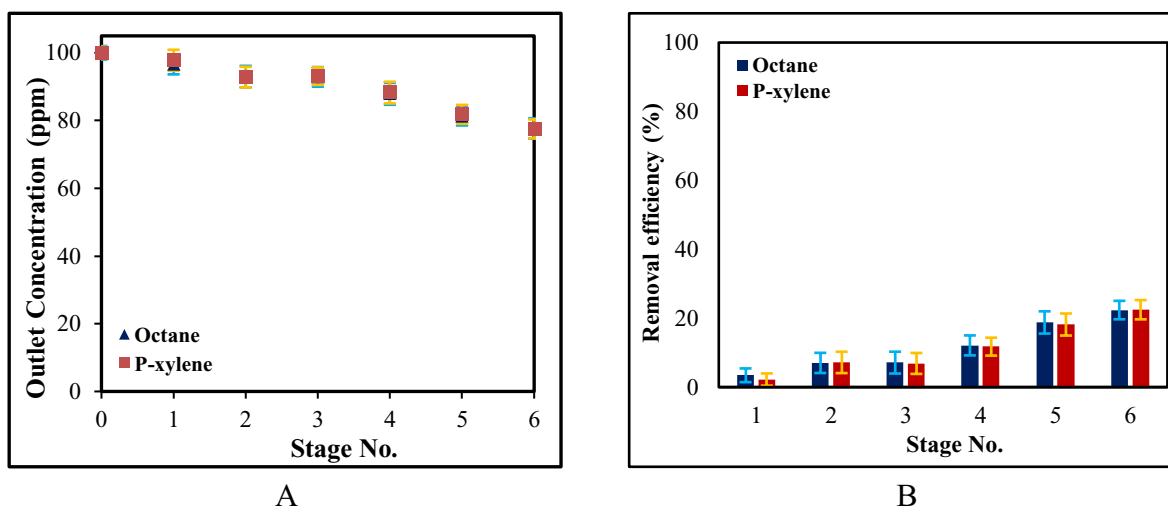
Figure 4.14. Effect of adsorbate aromaticity on the stage-wise outlet concentration and removal efficiency using ZEOCAT F603 where 0 is the inlet, 1 is the bottom stage, and 6 is the top stage of the fluidized bed (the error bars indicate the standard deviation of two tests)
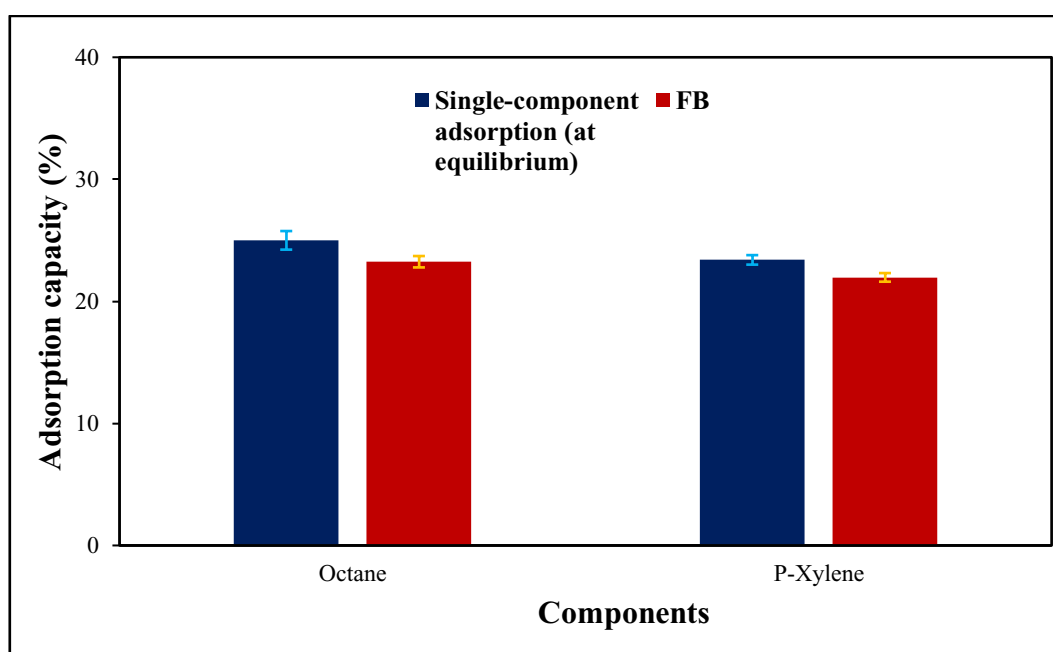

Figure 4.15. Comparison of the adsorption capacity at 100 ppm of octane and P-xylene on ZEOCAT F603 from the multicomponent test (the fluidized bed test) and the single component test (the error bars indicate the standard deviation of two tests)

4.5. Effect of boiling point

Boiling point is one of the properties of VOCs that can affect their adsorption (Li, et al., 2020). TMB and cumene were chosen to study the effect of boiling point on competitive adsorption in the fluidized bed reactor. The selected chemicals are isomers, and their

aromaticity, polarity, and molecular weight are similar, but their boiling point is different by approximately 20 ℃. This similarity helps one to observe the direct influence of the boiling point effect, within the range of 20 ℃, on the competitive adsorption.

It is noteworthy that analyzing the boiling point effect was essential for another reason. For the test of polarity, steric hindrance, and aromaticity, the VOCs' boiling point values were slightly different by 18, 11, and 13 ℃, respectively. The result from the boiling point test could confirm whether there was a correlation between the VOCs' boiling point and the obtained results in addition to the investigated effects in the previous tests. The results obtained from both adsorbents are presented in the following sections.

4.5.1. Kureha BAC G-70R test

As seen in **Figure 4.16**, the outlet concentration of each stage and the overall removal efficiency of the fluidized bed reactor for the two components was similar within the range of the boiling point difference. Both TMB and cumene showed a 97% removal efficiency in the multicomponent test.

Figure 4.17 presented the equilibrium adsorption capacity of TMB and cumene at 100 ppm. Similar to the multicomponent test, no meaningful difference was observed in the values of the equilibrium adsorption capacity of TMB and cumene.

The results suggest that the higher boiling point of TMB did not have an impact on its competitive adsorption with cumene. Stronger intermolecular forces were the introduced rationale for the preferable adsorption of VOCs with higher boiling points (Zhang et al., 2017). However, the adsorption of TMB did not seem to be favorable by it stronger intermolecular forces compared to cumene. It can be assumed that with up to a 20 ℃ difference in the boiling point of the VOCs, such a difference did not affect the VOCs' adsorption behavior. TMB and cumene are also isomers and share practically indistinguishable sets of properties such as

polarity, molecular weight, and aromaticity which might be another reason for their similar adsorption behavior on BAC.

Wang et. al. suggested the boiling point difference between the adsorbates as one of the influential factors on adsorption in a fixed bed reactor, using Kureha BAC G-70R as the adsorbent. However, the remarkable displacement and adsorption capacity occurred only for those components with a boiling point difference of greater than 20 °C (Wang, et al., 2012). Hence, the results from this test were consistent with their report of boiling point effect.

This result can also verify the correlation between the other effects and competitive adsorption in the fluidized bed using Kureha BAC G-70R. Since this range of boiling point difference is not influential on competitive adsorption, the observed difference between VOCs' adsorption capacities in other multicomponent tests (e.g., the effect of steric hindrance test) cannot be correlated to their slight boiling point dissimilarity.
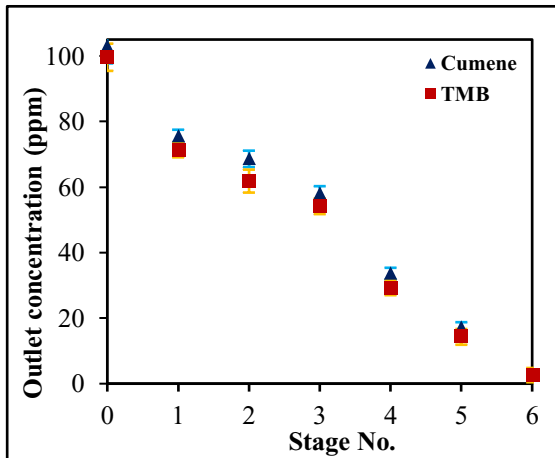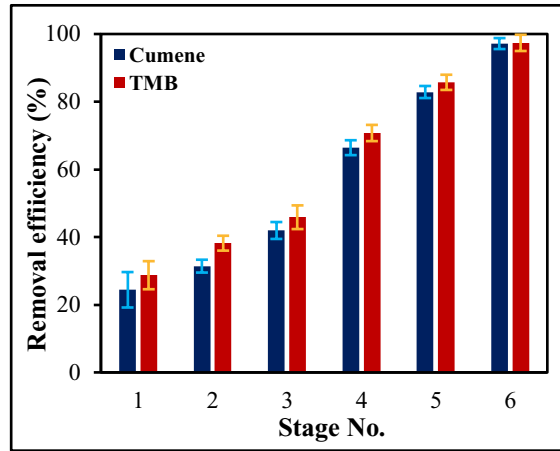
Figure 4.16. Effect of adsorbate boiling point on the stage-wise outlet concentration and removal efficiency using Kureha BAC G-70R where 0 is the inlet, 1 is the bottom stage, and 6 is the top stage of the fluidized bed (the error bars indicate the standard deviation of two tests)
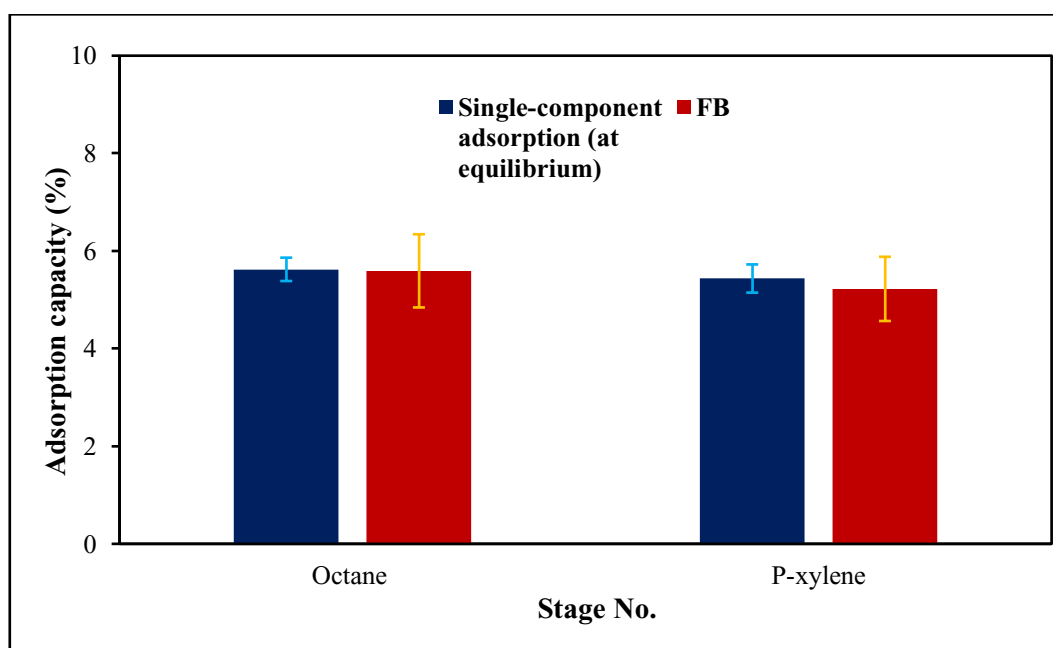

Figure 4.17. Comparison of the adsorption capacity at 100 ppm of TMB and cumene on Kureha BAC G-70R from the multicomponent test (the fluidized bed test) and the single component test (the error bars indicate the standard deviation of two tests)

4.5.2. ZEOCAT F603 test

The zeolite test showed a different behavior compared to BAC. First, the outlet concentration of each stage and the overall removal efficiency of the fluidized bed using ZEOCAT F603 (shown in **Figure 4.18**) were lower than of the Kureha BAC by 50%. The removal efficiency of the first two stages were zero since the zeolite was completely saturated.

Second, the equilibrium adsorption capacity of the TMB and cumene (**Figure 4.19**) was similar by approximately 6.5%. Similar to that of BAC, the zeolite had the same tendency toward TMB and cumene in their single component adsorption at 100 ppm.

Similar to BAC, the impact of the boiling point difference was not observed in the zeolite test. Intermolecular forces seem to be similar for both TMB and cumene in their adsorption onto the zeolite. With this range of boiling point difference and at the concentration of 100 ppm, the adsorbent-adsorbate interactions seemed to have been similar, resulting in a similar adsorption capacity. The high extent of similarity between these isomers seemed to outweigh their difference in their boiling point.

This can also justify the correlation between other investigated effects and competitive adsorption using this zeolite, as explained for BAC. The reported difference between VOCs' adsorption capacities in other multicomponent tests may not be correlated to their slight boiling point difference.

A   B
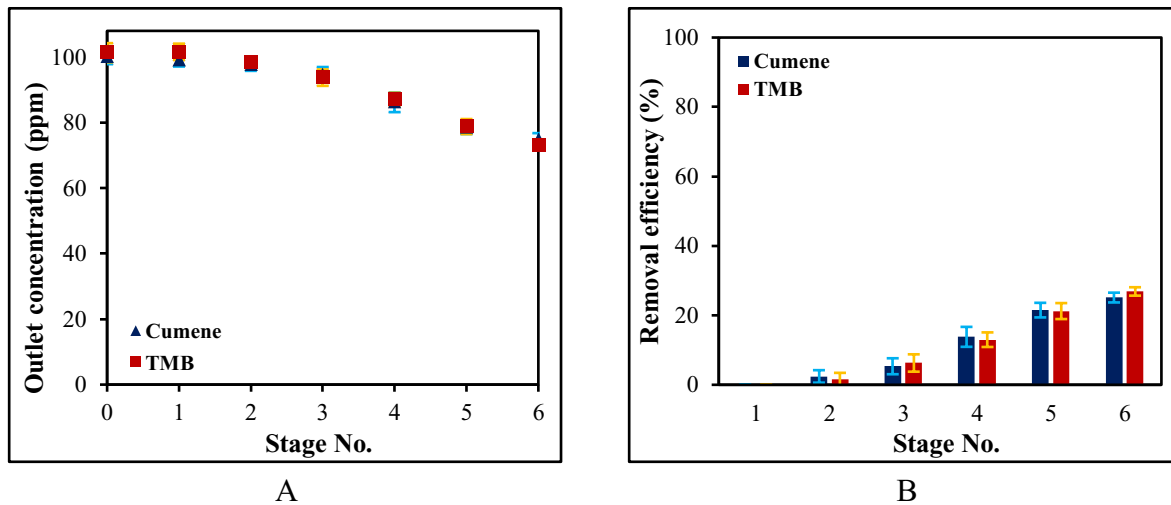
Figure 4.18. Effect of adsorbate boiling point on the stage-wise outlet concentration and removal efficiency using ZEOCAT F603 where 0 is the inlet, 1 is the bottom stage, and 6 is the top stage of the fluidized bed (the error bars indicate the standard deviation of two tests)
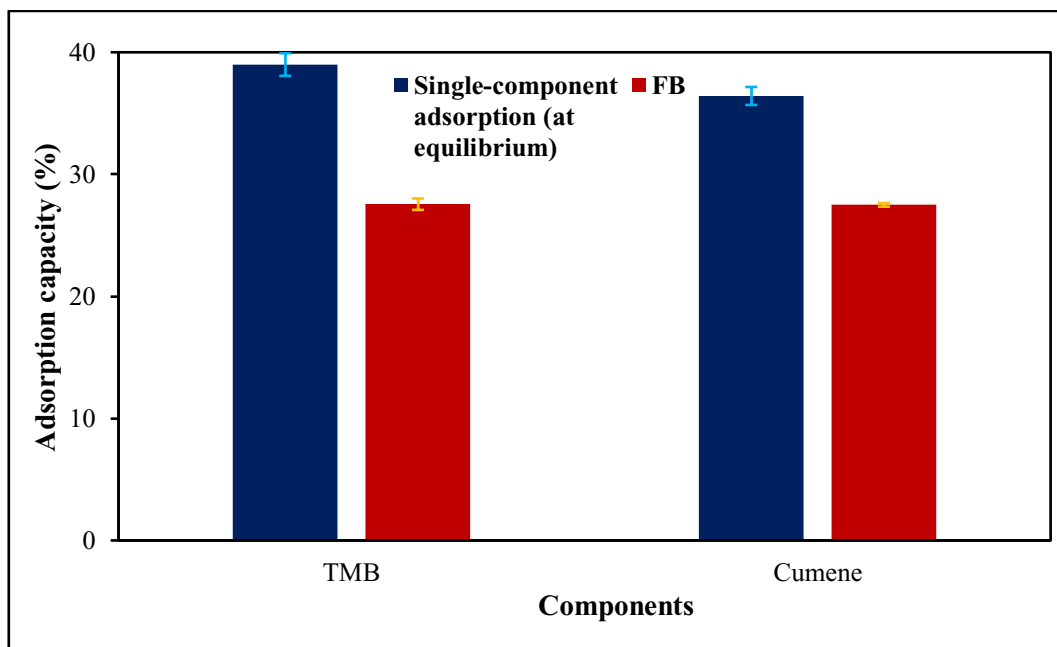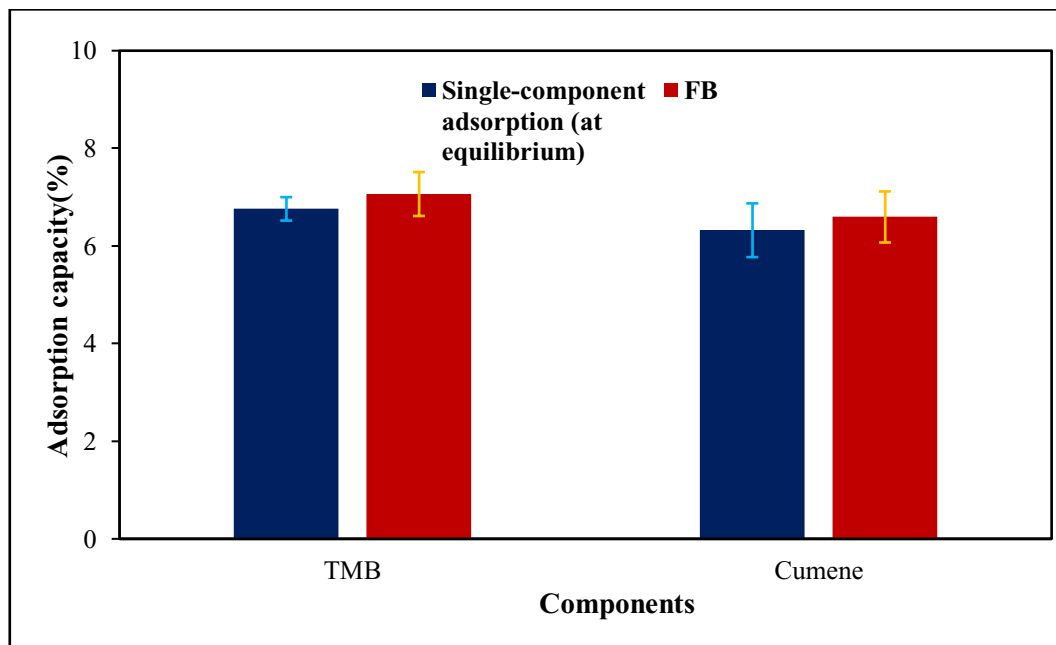

Figure 4.19. Comparison of the adsorption capacity at 100 ppm of TMB and cumene on ZEOCAT F603 from the multicomponent test (the fluidized bed test) and the single component test (the error bars indicate the standard deviation of two tests)

4.6. X-ray photoelectron spectroscopy (XPS):

X-ray photoelectron spectroscopy (XPS) test was carried out in order to determine the detailed chemical bonding on the surface of Kureha BAC G-70R. Knowing the bonds assists to indirectly verify the functional groups if they have certain signature bonds. **Figure 4.20** presents the results from the XPS test (the dotted black line was obtained directly from the test). Using the CasaXPS software, the deconvolution of the result was achieved, and the peaks of the colored curves represent the chemical bondings from the analysis.

The peaks corresponding to 286 eV and 288.4 eV, can be correlated to C−OH (hydroxyl) and COOH (carboxyl), respectively. The 286.8 eV peak, corresponding to C=O bond, might also be representative of carboxyl and carbonyl groups. The existence of oxygen-containing groups on the surface of BAC indicates the existence of hydrophilic sites on BAC surface. These sites facilitate the adsorption of polar compounds (Guo, et al., 2021; Meng et al., 2019). Elemental composition of the virgin BAC is presented in **Table 4.2**. O/C and (O + N)/C ratios can be indicators of hydrophilicity and polarity of the adsorbent surface, respectively. Based on the multicomponent test results for the effect of polarity (**Figure 4.2**), no difference in the adsorption of MIBK (polar) and heptane (non-polar) was observed using BAC. It can be assumed that the oxygen-containing groups available on BAC surface were not sufficient to impact the adsorption of the polar compound (Rajabi , et al., 2021; Meng et al., 2019).

The peak corresponding to approximately 284.7 eV, is attributed to the C=C bond on the surface of Kureha BAC G-70R, which could be ascribed to the graphitic carbon on the surface (Guo, et al., 2021; Yu, et al., 2014). Graphene existence can cause the π-electron donor-acceptor (π-EDA) interactions between aromatics and the adsorbents (Tan, et al., 2021). As discussed in the aromaticity section, BAC had a removal efficiency for the aromatic compound in the fluidized bed reactor test in the second, third, and fourth stage (**Figure 4.12**). In

accordance with the characteristics of BAC surface, it can be presumed that π-EDA interactions facilitated the adsorption of p-xylene in the middle stages (2,3, & 4). Other factors of the adsorbates, namely, molecular weight and polarity, are influential on competitive adsorption. Since p-xylene and octane are relatively similar in other physical/chemical properties, the overall removal efficiency of p-xylene in the multicomponent test was not influenced by its aromaticity and was similar to that of octane.
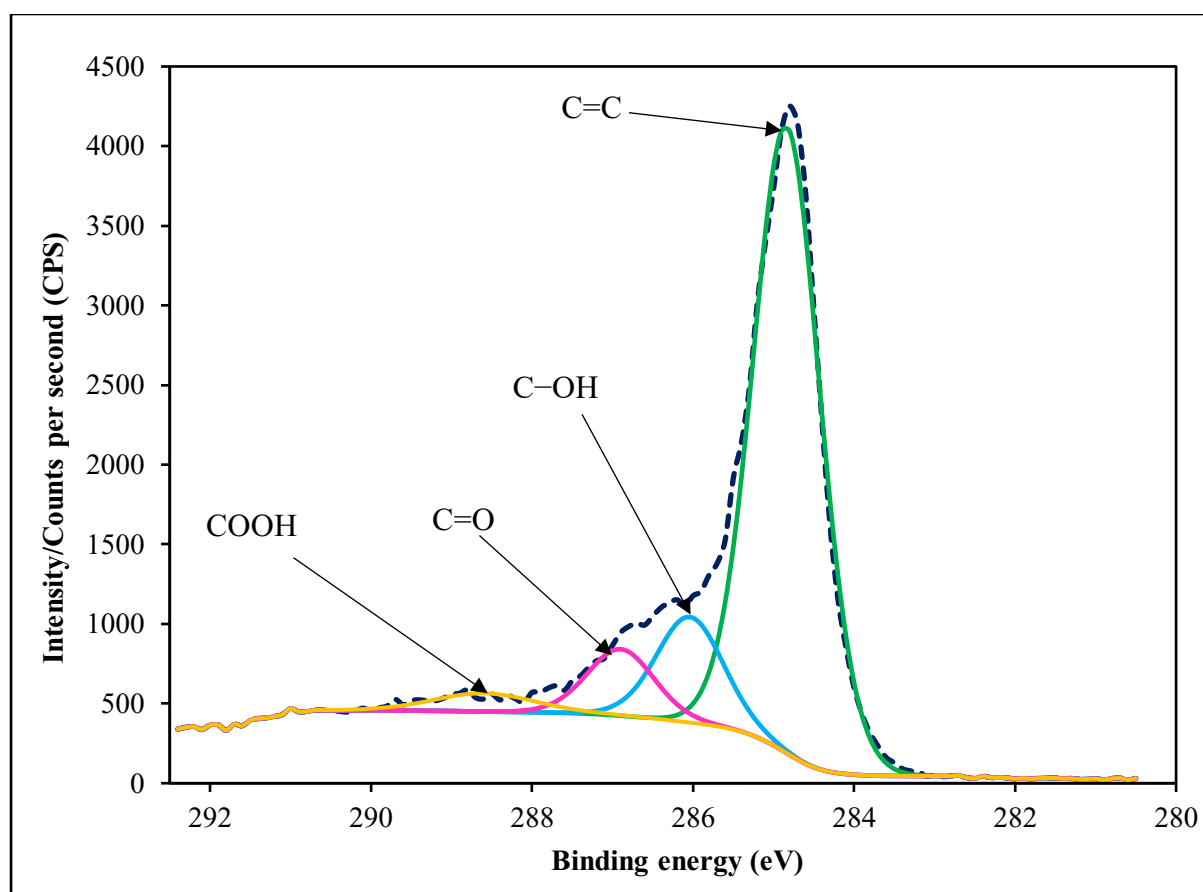
Figure 4.20. XPS result for virgin Kureha BAC G-70R

Table 4.2. Elemental composition of Virgin Kureha BAC G-70R (Kamravaei, 2014)

Element	Mass concentration	Atomic concentration
C	93.2	94.8
O	6.5	5.0
N	0.3	0.2

Chapter 5: Conclusion and recommendations

5.1. Conclusion

The effect of polarity, steric hindrance, aromaticity, and boiling point were investigated using a beaded activated carbon (Kureha BAC G-70R) and a beaded zeolite (ZEOCAT F603) in a multi-stage countercurrent fluidized bed reactor. Methyl isobutyl ketone and heptane, hexane and cyclohexane, p-xylene and octane, and TMB and cumene were the four pairs of VOCs used for the tests which targeted the effect polarity, steric hindrance, aromaticity, and boiling point, respectively.

BAC had a similar removal efficiency for MIBK and heptane which indicated that BAC did not favor the adsorption of the polar component. This might be attributed to the low content of oxygen-containing groups (low number of hydrophilic sites) on BAC surface. Similarly, with up to an approximately 20 ℃ difference in VOCs' boiling point, such a difference did not affect the competitive adsorption as BAC showed a similar uptake of TMB and cumene. Steric hindrance, and aromaticity of the adsorbates, however, seemed to have an impact on competitive adsorption on BAC. Between hexane and cyclohexane, it is presumed that the adsorption of cyclohexane on BAC was hindered due to its molecular structure, while the adsorption of hexane onto the microporous structure of the adsorbent was facilitated due to its linear structure. Further, BAC had a greater affinity for the aromatic compound in the second, third, and fourth stages of the fluidized bed reactor possibly due to the π-π interaction of the aromatic compound and BAC surface. In stages 5 and 6, the fresh BAC seemed to have a sufficient capacity for obtaining a similar removal efficiency for the VOCs, while as the adsorbent became more saturated in the lower stages, it showed a greater affinity for the aromatic compound.

On the other hand, the zeolite had a higher adsorption capacity for MIBK compared to heptane, which suggested the greater affinity of the zeolite for the polar compound. This can also

indicate the low Si/Al ratio of ZEOCAT F603. Steric hindrance effect had a drastic impact on competitive adsorption of hexane and cyclohexane onto the zeolite. The adsorption of cyclohexane was completely restrained by hexane which presumably stemmed from cyclohexane molecular structure and conformations, and the zeolite framework. Aromaticity and boiling point, on the other hand, did not influence the competitive adsorption as the zeolite did not show a greater affinity toward the aromatic compound nor the compound with a higher boiling point. **Table 5.1** summarizes the findings about competitive adsorption from this research.

Table 5.1. Summary of the multicomponent tests in the fluidized bed

Target effect	Adsorbates	Adsorbent	Effect seen on competitive adsorption
Polarity	MIBK & heptane	BAC Kureha G-70R	No
Polarity	MIBK & heptane	ZEOCAT F603	Yes
Steric hindrance	Hexane & cyclohexane	BAC Kureha G-70R	Yes
Steric hindrance	Hexane & cyclohexane	ZEOCAT F603	Yes
Aromaticity	p-xylene & octane	BAC Kureha G-70R	Yes
Aromaticity	p-xylene & octane	ZEOCAT F603	No
Boiling point (20 ℃) difference	TMB & cumene	BAC Kureha G-70R	No
Boiling point 20 ℃) difference	TMB & cumene	ZEOCAT F603	No

Further, the adsorption isotherm tests were obtained for each VOC using both adsorbents. Kureha BAC G-70R showed a higher equilibrium adsorption capacity for all the VOCs within the concentration range of 50 to 1000 ppm compared to ZEOCAT F603 due to its higher surface area, and micropore and total pore volume. TMB had the highest adsorbed

amount on BAC, while MIBK had the highest value on the zeolite within the concentration of 50 to 1000 ppm. The adsorbed amount of cyclohexane at equilibrium was noticeably lower within the entire range of the concentration values using the zeolite which might be attributed to cyclohexane's structure and conformations and the framework of the zeolite.

5.2. Recommendations

Having done this research, the list below represents the recommendations for future research:

- Additional factors such as the molecular weight and saturated vapor pressure can be also analyzed on competitive adsorption of VOCs in fluidized beds.

- The effect of boiling point was only studied with the range of approximately 20 ℃ difference. Higher boiling point difference between VOCs can be studied for a more comprehensive result.

- All the mixtures prepared for this study were binary. A mixture of more VOCs can be analyzed in order to investigate the effects of adsorbates' properties.

- All the multicomponent tests in this study were carried out using dry air as carrier gas. Adsorbate's properties effects can be investigated with a humid air stream which is more realistic.

References

Al-Ghouti, M. A., & da'ana, D. A. (2020). Guidelines for the use and interpretation of adsorption isotherm models: A review. *Journal of Hazardous Materials, 393*, 122383.

Amdebrhan, B. T. (2018). Evaluating the Performance of Activated Carbon, Polymeric, and Zeolite Adsorbents for Volatile Organic Compounds. *Master's thesis, University of Alberta, Edmonton, Canada*.

Andrews, W. G. (1890). *United States of America Patent No. 426092.*

Baerlocher, C., L.B., M., & Olson, D. (2007). *Atlas of zeolite framework types.* Elsevier.

Bansal , R. C., & Goyal , M. (2005). *Activated Carbon Adsorption.* CRC Press.

Bell, J. G., Zhao, X., Uygur, Y., & Mark Thomas, K. (2011). Adsorption of Chloroaromatic Models for Dioxins on Porous Carbons: The Influence of Adsorbate Structure and Surface Functional Groups on Surface Interactions and Adsorption Kinetics. *The Journal of Physical Chemistry C, 115*, 2776–2789.

Benkhedda, J., Jaubert, J.-N., & Barth, D. (2000). Experimental and Modeled Results Describing the Adsorption of Toluene onto Activated Carbon. *Journal of Chemical and Engineering Data, 45*, 650-653.

Blocki, S. W. (1993). Hydrophobic zeolite adsorption: A proven advancement in solvent separation technology. *Environmental Progress, 12*, 226–237.

Boulinguiez, B., & Le Cloirec, P. (2010). Adsorption on activated carbons of five selected volatile organic compounds present in biogas: Comparison of granular and fiber cloth materials. *Energy and Fuels, 24*, 4756-4765.

Bozbiyik, B., Duerinck, T., Lannoeye, J., De Vos, D. E., Baron, G. V., & Denayer, J. F. (2014). Adsorption and separation of n-hexane and cyclohexane on the UiO-66 metal–organic framework. *Microporous and Mesoporous Material, 183*, 143–149.

Brauner, S., Emmett, P. H., & Teller, E. (1938). Adsorption of Gases in Multimolecular Layers. *Journal of the American Chemical Society, 60*, 309–319.

Calleja, G., Pau, J., & Calles, J. A. (1998). Pure and Multicomponent Adsorption Equilibrium of Carbon Dioxide, Ethylene, and Propane on ZSM-5 Zeolites with Different Si/Al Ratios. *Journal of Chemical and Engineering Data, 43*, 994-1003.

Cavalcante, C., & Ruthven, D. (1995). Adsorption of branched and cyclic paraffins in silicalite equilibrium. *Industrial & Engineering Chemistry Research, 34*, 177-184.

Chiang, B.-C., Wey, M.-Y., & Yang, W.-Y. (2000). Control of Incinerator Organics by Fluidized Bed Activated Carbon Adsorber. *Journal of Environmental Engineering, 126*, 985-992.

Chiang, Y.-C., Chiang, P.-C., & Huang, C.-P. (2001). Effects of pore structure and temperature on VOC adsorption on activated carbon. *Carbon, 39*, 523-534.

Clayden, J., Greeves, N., & Warren, S. (2001). *Organic Chemistry* . Oxford: Oxford University Press.

Davarpanah, M. (2020). Modeling the Performance and Hydrodynamic Behavior of a Countercurrent Multistage Fluidized Bed Adsorber. *Doctor of Philosophy, University of Alberta, Edmonton, Canada*.

Davarpanah, M., Hashisho, Z., Phillips, J., Compton, D., Anderson, J., & Nichols, M. (2020). Modeling VOC adsorption in a multistage countercurrent fluidized bed adsorber. *Chemical Engineering Journal, 394*.

Denayer, J., Bouyermaouen, A., & Baron, G. (1998). Adsorption of Alkanes and Other Organic Molecules in Liquid Phase and in the Dense Vapor Phase: Influence of Polarity, Zeolite Topology, and External Fluid Density and Pressure. *Industrial & Engineering Chemistry Research, 37*, 3691-3698.

Diaz, E., Salvador, O., Vega, A., & Coca, J. (2004). Adsorption characterisation of different volatile organic compounds over alumina, zeolites and activated carbon using inverse gas chromatography. *Journal of Chromatography A, 1049*, 139-146.

Dobre, T., Pârvulescu, O., Iavorschi, G., Stroescu, M., & Stoica, A. (2014). Volatile Organic Compounds Removal from Gas Streams by Adsorption onto Activated Carbon. *Industrial & Engineering Chemistry Research, 53*, 3622−3628.

Dolidovich, A., Akhremkova, G., & Efremtsev, V. (1999). Novel Technologies of VOC Decontamination in Fixed, Moving and Fluidized Catalyst-Adsorbent Beds. *The Canadian Journal of Chemical Engineering, 77*, 342-355.

Fletcher, A., Yüzak, Y., & Thomas, K. (2006). Adsorption and desorption kinetics for hydrophilic and hydrophobic vapors on activated carbon. *Carbon, 44*, 989-1004.

Geldart, D. (1973). Types of Gas Fhidization. *Powder Technology, 7*, 285-292.

Ghoshal , A. K., & Manjare, S. D. (2002). Selection of appropriate adsorption technique for recovery of VOCs: an analysis. *Loss Prevention in the Process Industries*, 413–421.

Giraudet, S., Boulinguiez, B., & Le Cloirec, P. (2014). Adsorption and electrothermal desorption of volatile organic compounds and siloxanes onto an activated carbon fiber cloth for biogas purification. *Energy Fuels, 28*(6), 3924–3932.

Government of Canada. (2013, 07 17). *Common air pollutants: volatile organic compounds*. Retrieved from https://www.canada.ca/en/environment-climate-change/services/air-pollution/pollutants/common-contaminants/volatile-organic-compounds.html

Government of Canada. (2017, 06 22). *Volatile organic compounds in products overview*. Retrieved from https://www.canada.ca/en/environment-climate-change/services/managing-pollution/sources-industry/volatile-organic-compounds-consumer-commercial/overview.html

Government of Canada. (2021, 06 29). *Automotive refinishing products and volatile organic compounds*. Retrieved from https://www.canada.ca/en/environment-climate-change/services/managing-pollution/sources-industry/volatile-organic-compounds-consumer-commercial/automotive-refinishing-products.html

Government of Canada. (2021). *Renewal of the Federal Agenda on the Reduction of Volatile Organic Compound (VOC) Emissions from Consumer and Commercial Products for the 2021 to 2028 period: discussion paper.*

Government of Canada. (2021, 06 21). *Toxic substances list: schedule 1*. Retrieved from https://www.canada.ca/en/environment-climate-change/services/canadian-environmental-protection-act-registry/substances-list/toxic/schedule-1.html

Government of Canada, Environment and Climate Change. (2019). *Canada's Air Pollutant Emissions Inventory Report.*

Guenther, A., Hewitt, C., Erickson, D., Fall, R., Geron, C., Graedel, T., Harley, P., Klinger, L., Lerdau, M., McKay, W.A., Pierce, T.; Scholes, B., Stienbrecher, R., Tallamraju, R., Taylor, R., Zimmerman, P. (1995, May 20). A global model of natural volatile organic compoundemissions. *Journal of Geophysical Research, 100*, 8873-8892.

Guo, J., Kang, L., Lu, X., Zhao, S., Li, J., Shearing, P. W., Wang, R., Brett, D.J.L., He, G., Chai, G., Parkin, I. (2021). Self-activated cathode substrates in rechargeable zinc–air batteries. *Energy Storage Materials, 35*, 530-537.

Guth, J.-L., & Henri, K. (1999). Synthesis of Aluminosilicate Zeolites and Related Silica-Based Materials. In J. Weitkamp, & L. Puppe, *Catalysis and Zeolites; Fundamentals and Applications.* New York, Germany: Springer-Verlag Berlin Heidelberg.

Guy, O., & Walker, K.-A. (2016). Graphene Functionalization for Biosensor Applications. In S. Saddow, *Silicon Carbide Biotechnology.* Elsevier.

Hamed, A., Abd-El-Rahman, W., & El-Emam, S. (2010). Experimental study of the transient adsorption/desorption characteristics of silica gel particles in fluidized bed. *Energy, 35*, 2468-2483.

Hashisho, Z., Emamipour, H., Rood, M., Hay, K., Kim, B., & Thurston, D. (2008). Concomitant Adsorption and Desorption of Organic Vapor in Dry and Humid Air Streams using Microwave and Direct Electrothermal Swing Adsorption. *Environmental Science and Technology, 42*, 9317-9322.

Hashisho, Z., Rood, M., & Botich, L. (2005). Microwave-Swing Adsorption To Capture and Recover Vapors from Air Streams with Activated Carbon Fiber Cloth. *Environmental Science and Technology, 39*, 6851-6859.

Hoskins, B. F., & Robson, R. (1989). Infinite Polymer Frameworks Consisting of Three Dimensionally Linked Rod-like Segments. *American Chemical Society, 111*, 5962–5964.

Huddersman, K., & Klimczyk, M. (1996). Separation of Branched Hexane Isomers Using Zeolite Molecular Sieves. *AIChE Journal, 42*, 405-408.

Hung, H.-W., & Lin, T.-F. (2007). Prediction of the Adsorption Capacity for Volatile Organic Compounds onto Activated Carbons by the Dubinin–Radushkevich–Langmuir Model. *Air & Waste Management Association, 57*, 497-506.

Inglezakis, V. (2006). *Adsorption, Ion Exchange, and Catalysis: Design of Operations and Environmental Applications.* Elsevier Science.

Jain, J. S., & Snoeyink, V. L. (1973). Adsorption from bisolute systems on active carbon. *Water Pollution Control Federation, 45*, 2463-2479.

Kamravaei, S. (2014). Effect of fluidization on adsorption of volatile organic compounds on beaded activated carbon. *Master's thesis, University of Alberta, Edmonton, Canada*.

Kamravaei, S., Shariaty, P., Lashaki, M. J., Atkinson, J. D., Hashisho, Z., Philips, J. H., Anderson, James E, Nichols, M. (2017). Effect of Beaded Activated Carbon Fluidization on Adsorption of Volatile Organic Compounds. *Industrial & Engineering Chemistry Research, 56*, 1297−1305.

Keenan, J., Chao, J., & Kaye, J. (1992). *Gas Tables: International Version : Thermodynamic Properties of Air Products of Combustion and Component Gases Compressible Flow Functions.* Krieger Publishing Company.

Keller, J., & Staudt, R. (2005). *Gas Adsorption Equilibria; Experimental methods and Adsorptive Isotherms.* Boston: Springer Science + Business Media, Inc.

Khan, F. I., & Ghoshal, A. K. (2000). Removal of Volatile Organic Compounds from polluted air. *Loss Prevention in the Process Industries, 13*, 527–545.

Kim, B. (2011). VOC Emissions from Automotive Painting and Their Control: A Review. *Environmetal Engineering Research, 16*, 1-9.

Kunii, D., & Levenspiel, O. (1991). *Fluidization Engineering.* Butterworth—Heinemann.

Lachet, V., Boutin, A., Tavitian, B., & Fuchs, A. (1999). Molecular Simulation of p-Xylene and m-Xylene Adsorption in Y Zeolites. Single Components and Binary Mixtures Study. *Langmuir, 15*, 8678-8685.

Langmuir, I. (1916). The Constitution and Fundamental Properties of Solids and Liquids. *Journal of the American Chemical Society, 38*, 2221–2295.

Larsen, E., & Pilat, M. (1991). Design and Testing of a Moving Bed VOC Adsorption System. *Environmental Progress*, 75-82.

Larsen, E., & Pilat, M. (1991). Moving Bed Adsorption System for Control of VOCs from an Aircraft Painting Facility. *Air and Waste Management Association, 41*, 1199-1206.

Lashaki, M. J., Atkinson, J. D., Hashisho, Z., Philips, J. H., Anderson, J. E., & Nichols, M. (2016). The role of beaded activated carbon's pore size distribution on heel formation during cyclic adsorption/desorption of organic vapors. *Journal of Hazardous Materials, 315*, 42–51.

Lashaki, M., Fayaz, M., Wang, H., Hashisho, Z., Philips, J., Anderson, J., & Nichols, M. (2012). Effect of Adsorption and Regeneration Temperature on Irreversible Adsorption of Organic Vapors on Beaded Activated Carbon. *Environmental Science & Technology, 46*, 4083−4090.

Lashaki, M., Hashisho, Z., J.H., P., Crompton, D., Anderson, J., & Nichols, M. (2020). Mechanisms of heel buildup during cyclic adsorption-desorption of volatile organic compounds in a full-scale adsorber-desorber. *Chemical Engineering Journal, 400*, 124937.

Laskar, I. I., & Hashisho, Z. (2020). Insights into modeling adsorption equilibria of single and multicomponent systems of organic and water vapors. *Separation and Purification Technology, 241*, 116681.

Lee, M.-G., Lee, S.-W., & Lee, S.-H. (2006). Comparison of vapor adsorption characteristics of acetone and toluene based on polarity in activated carbon fixed-bed reactor. *Korean Journal of Chemical Engineering, 23*, 773-778.

Leslie, G. (2000, 04 29). Health Risks from Indoor Air Pollutants: Public Alarm and Toxicological Reality. *Indoor Built Environment, 9*, 5-16.

Li, J.-R., Kuppler, R., & Zhou, H.-C. (2009). Selective gas adsorption and separation in metal–organic frameworks. *Chemical Society Reviews, 38*, 1477-1504.

Li, X., Zhang, L., Yang, Z., Wang, P., Yan, Y., & Ran, J. (2020). Adsorption materials for volatile organic compounds (VOCs) and the key factors for VOCs adsorption process: A review. *Separation and Purification Technology, 235*, 116213.

Lillo-Rodenas, M. A., Fletcher, A. J., Thomas, K. M., Cazorla-Amorós, D., & Linares-Solano, A. (2006). Competitive adsorption of a benzene–toluene mixture on activated carbons at low concentration. *Carbon, 44*, 1455–1463.

Limousin, G., Gaudet, J. -P., Charlet, L., Szenknect, S., Barthes, V., & Krimissa, M. (2007). Sorption isotherms: A review on physical bases, modeling and measurement. *Applied Geochemistry, 22*, 249–275.

Lin, D., & Xing, B. (2008). Adsorption of Phenolic Compounds by Carbon Nanotubes: Role of Aromaticity and Substitution of Hydroxyl Groups. *Environmental Science and Technology, 42*, 7254–7259.

Long , C., Liu, P., Li, Y., Li, A., & Zhang, Q. (2011). Characterization of Hydrophobic Hypercrosslinked Polymer as an Adsorbent for Removal of Chlorinated Volatile Organic Compounds. *Environmental Science and Technology, 45*, 4506–4512.

Mather, R. (2009). Surface modification of textiles by plasma treatments. In Q. Wei, *Surface Modification of Textiles.* Woodhead Publishing.

Meng, F., Song, M., Wei, X., & Wang, Y. (2019). The contribution of oxygen-containing functional groups to the gas-phase adsorption of volatile organic compounds with different polarities onto lignin-derived activated carbon fibers. *Environmental Science and Pollution Research, 26*, 7195–7204.

Missen, R., Mims, C., & Saville, B. (1999). *Introduction to chemical reaction engineering and kinetics.* Wiley New York.

Mohanty, C., & Meikap, B. (2011). Modeling the operation of a three-stage fluidized bed reactor for removing CO2 from flue gases. *Journal of Hazardous Materials, 187*, 113–121.

Mohanty, C., Malavia, G., & Meikap, B. (2009). Development of a Countercurrent Multistage Fluidized-Bed Reactor and Mathematical Modeling for Prediction of Removal Efficiency of Sulfur Dioxide from Flue Gases. *Industrial & Engineering Chemistry Research, 48*, 1629–1637.

Monneyron, P., Manero, M., & Foussard, J. (2003). Measurement and Modeling of Single- and Multi-Component Adsorption Equilibria of VOC on High-Silica Zeolites. *Environmental Science and Technology, 37*, 2410-2414.

Myers, A. L., & Prausnitz, J. M. (1965). Thermodynamics of Mixed-Gas Adsorption. *AIChE Journal, 11*, 121-127.

Nevskaia, D., Castillejos-lopez, E., Munoz, V., & Guerrero-ruiz, A. (2004). Adsorption of Aromatic Compounds from Water by Treated Carbon Materials. *Environmental Science and Technology, 38*, 5786-5796.

Ouzzine, M., Romero-Anaya, A. J., Lillo-Rodenas, M. a., & Linares-Solano, A. (2019). Spherical activated carbons for the adsorption of a real multicomponent VOC mixture. *Carbon, 148*, 214-223.

Papasavva, S., Kia, S., Claya, J., & Gunther, R. (2001). Characterization of automotive paints: an environmental impact analysis. *Progress in Organic Coatings, 43*, 193-206.

Paredes-Doig, A., Sun-Kou, M., Picasso-Escobar, G., & Lazo, J. (2014). A Study of the Adsorption of Aromatic Compounds Using Activated Carbons Prepared from Chestnut Shell. *Adsorption Science and Technology, 32*, 2-3.

Pariselli, F., Sacco, M., Ponti, J., & Rembges, D. (2009). Effects of toluene and benzene air mixtures on human lung cells (A549). *Experimental and Toxicologic Pathology, 61*, 381–386.

Parmar, G., & Rao, N. (2009). Emerging Control Technologies for Volatile Organic Compounds. *Environmental Science and Technology, 39*, 41-78.

Pasti, L., Rodeghero, E., Sarti, E., Bosi, V., Cavazzini, A., Bagatin, R., & Martucci, A. (2016). Competitive adsorption of VOCs from binary aqueous mixtures on zeolite ZSM-5. *The Royal Society of Chemistry, 6*, 54544–54552.

Peralta, D., Chaplais, G., Simon-Masseron, A., Barthelet, K., Chizallet, C., Quoineaud, A., & Pirngruber, G. (2012). Comparison of the Behavior of Metal−Organic Frameworks and Zeolites for Hydrocarbon Separations. *Journal of the American Chemical Society, 134*, 8115-8126.

Philippsen, C., Vilela, A., & Zen, L. (2015). Fluidized bed modeling applied to the analysis of processes: review and state of the art. *Journal of Materials Research and Technology, 4*, 208–216.

Pui, W., Yusoff, R., & Aroua, M. (2018). A review on activated carbon adsorption for volatile organic compounds (VOCs). *Reviews in Chemical Engineering, 35*, 649-668.

Rüdisüli, M., Schildhauer, T., Biollaz, S., & Ruud van Ommen, J. (2012). Scale-up of bubbling fluidized bed reactors — A review. *Powder Technology, 217*, 21-38.

Rajabi , H., Mosleh, M. H., Prakoso, T., Ghaemi, N., Mandal, P., Lea-Langton, A., & Sedighi, M. (2021). Competitive adsorption of multicomponent volatile organic compounds on biochar. *Chemosphere*, 131288.

Rodriguez-Reinoso, F., Molina-Sabio, M., & Muñecas, M. (1992). Effect of Microporosity and Oxygen Surface Groups of Activated Carbon in the Adsorption of Molecules of Different Polarity. *The Journal of Physical Chemistry, 96*, 2707-2713.

Romero-Anaya, A. J., Lilo-Rodenas, M. A., & Linares-Solano, A. (2015). Factors governing the adsorption of ethanol on spherical activated carbons. *Carbon, 83*, 240-249.

Romero-Anaya, A., Lillo-Rodenas, M., & Linares-Solano, A. (2010). Spherical activated carbons for low concentration toluene adsorption. *Carbon, 48*, 2625-2633.

Rouquerol, F., Rouquerol, J., & Sing, K. (1998). *Adsorption by Powders and Porous Solids.* Marseille: Academic Press.

Roy, S., Mohanty, C. R., & Meikap, B. C. (2009). Multistage fluidized bed reactor performance characterization for adsorption of carbon dioxide. *Industrial and Engineering Chemistry Research, 48*, 10718-10727.

Sampieri, A., Perez_Osorio, G., Hernández-Espinosa, M. A., Ruiz-López, I. I., Ruiz-Reyes, M., Arriola-Morales, J., & Narváez-Fernández, R. I. (2018). Sorption of BTEX on a nanoporous composite of SBA-15 and a calcined hydrotalcite. *Nano Convergence*, 5-21.

Saxena, S., & Vadivel, R. (1988). Wall effects in gas-fluidized beds at incipient fluidization. *The Chemical Engineering Journal, 39*, 133-137.

Shariaty, P., Kamravaei, S., Atkinson, J., Hashisho, Z., Philips, J., Anderson, J., Nichols, M., Crompton, D. (2015). Effect of Operational Parameters on the Performance of a Multistage Fluidized Bed Adsorber. *AIChE Annual Meeting.*

Shen, W., Li, Z., & Liu, Y. (2008). Surface Chemical Functional Groups Modification of Porous Carbon. *Recent Patents on Chemical Engineering, 1*, 27-40.

Shirzad, M., Karimi, M., Silva, J., & Rodrigues, A. (2019). Moving Bed Reactors: Challenges and Progress of Experimental and Theoretical Studies in a Century of Research. *Industrial & Engineering Chemistry Research, 58*, 9179−9198.

Shwanke, A., Balzer, R., & Pergher, S. (2012). Microporous and Mesoporous Materials from Natural and Inexpensive Sources. In *Handbook of Ecomaterials.* Springer, Cham.

Silva , P., Vilela, S. F., Tome, J. C., & Almeida Paz, F. A. (2015). Multifunctional metal–organic frameworks: from academia to industrial applications. *The Royal Society of Chemistry, 44*, 6774--6803.

Slawek, A., Grzybowska, K., Vicent-Luna, J., Makowsk, W., & Calero, S. (2018). Adsorption of Cyclohexane in Pure Silica Zeolites: High-Throughput Computational Screening Validated by Experimental Data. *ChemPhysChem, 19*, 3364-3371.

Song, W., Tondeur, D., Luo, L., & Li, J. (2005). VOC Adsorption in Circulating Gas Fluidized Bed. *Adsorption, 11*, 853-858.

Suwanayuen, S., & Danner, R. P. (1980). Vacancy solution theory of adsorption from gas mixtures. *AIChE Journal, 26*, 76-83.

Suzuki, M. (1989). *Adsorption Engineering.* Tokyo: Elsevier Science Ltd.

Tan, X.-F., Zhu, S.-S., Wang, R.-P., Chen, Y.-D., Show, P.-L., Zhang, F.-F., & Ho, S.-H. (2021). Role of biochar surface characteristics in the adsorption of aromatic compounds: Pore structure and functional groups. *Chinese Chemical Letters, 32*, 2939–2946.

Tang, H., Zhao, Y., Shan, S., Yang, Y., Liu, D., Cui, F., & Xing, B. (2018). Theoretical insight into the adsorption of aromatic compounds on graphene oxide. *Environmental Science: Nano, 5*, 2357–2367.

Tefera, D. T., Hashisho, Z., Philips, J. H., Anderson, J. E., & Nichols, M. (2014). Modeling Competitive Adsorption of Mixtures of Volatile Organic Compounds in a Fixed-Bed of Beaded Activated Carbon. *Environmental Science and Technology*, 5108−5117.

U.S. Department of Health and Human Services. (2016). *14th Report on Carcinogens.* U.S. Department of Health and Human Services. Retrieved from https://ntp.niehs.nih.gov/go/roc14

Van lare, C. (1991). Mass transfer in gas fluidized beds: scaling, modeling and particle size influence. *Technische Universiteit Eindhoven*.

Varma, Y. (1975). Pressure Drop of the Fluid and the Flow Patterns of the Phases in Multistage Fluidisation. *Powder Technology, 12*, 167-174.

Villacañas, F., Pereira, M., Órfão, J., & Figueiredo, J. (2006). Adsorption of simple aromatic compounds on activated carbons. *Journal of Colloid and Interface Science, 293*, 128–136.

Wang, C.-W., Chang, K.-S., & Chung, T.-W. (2004). Adsorption Equilibria of Aromatic Compounds on Activated Carbon, Silica Gel, and 13X Zeolite. *Journal of Chemical and Engineering Data, 49*, 527-531.

Wang, G., Dou, B., Wang, J., Wang, W., & Hao, Z. (2013). Adsorption properties of benzene and water vapor on hyper-cross-linked polymers. *The Royal Society of Chemistry, 3*, 20523–20531.

Wang, H., Lashaki , M. J., Fayaz, M., Hashisho, Z., Philips, J. H., Anderson, J. E., & Nichols, M. (2012). Adsorption and Desorption of Mixtures of Organic Vapors on Beaded Activated Carbon. *Environmental Science and Technology*, 8341−8350.

Wang, Q., Liang, X. Y., Zhang, R., Liu, C. J., Liu, X. J., Qiao, W. M., Zhan, L., Ling, L. C. (2009). Preparation of polystyrene-based activated carbon spheres and their adsorption of dibenzothiophene. *New Carbon Materials, 24*, 55-59.

Webster, C., Drago, R., & Zerner, M. (1998). Molecular Dimensions for Adsorptives. *Journal of the American Chemical Society, 120*, 5509-5516.

Weitkamp, J. (2000). Zeolites and catalysis. *Solid State Ionics, 131*, 175-188.

Wu, Q., Huang, W., Wang, H.-J., Pan, L.-L., Zhang, C.-L., & Liu, X.-K. (2015). Reversely Swellable Porphyrin-linked Microporous Polyimide Networks with Super-adsorption for Volatile Organic Compounds. *Chinese Journal of Polymer Science, 33*, 1125-1132.

Xu, W., Dong, J., Li, J., Li, J., & Wu, F. (1990). A Novel Method for the Preparation of Zeolite ZSM-5. *Journal of the Chemical Society, Chemical Communications*, 755-756.

Yan, Z., Ma, D., Zhuang, J., Liu, X., Liu, X., Han, X., Bao, X., Chang, F., Xu, L., Liu, Z. (2003). On the acid-dealumination of USY zeolite: a solid state NMR investigation. *Journal of Molecular Catalysis A, 194*, 153-167.

Yang, R. T. (1987). *Gas Separation by Adsorption Processes.* New York: Butterworth.

Yang, W.-C. (2003). Bubbling Fluidized Beds. In W.-C. Yang, *Handbook of Fluidization and Fluid-particle systems.* Taylor & Francis Group LLC.

Yang, X., Yi, H., Tang, X., Zhao, S., Yang, Z., & Ma, Y., Feng, T., Cui, X. (2018). Behaviors and kinetics of toluene adsorption-desorption on activated carbons with varying pore structure. *Journal of Environmental Sciences, 67*, 104-114.

Yanxu, L., Jiangyao, C., & Yinghuang, S. (2008). Adsorption of multicomponent volatile organic compounds on semi-coke. *Carbon, 46*, 858–863.

Yates, J., & Mullin, J. (1983). *Fundamentals of Fluidized-bed Chemical Processes.* London: Butterworths Monographs in Chemical Engineering.

Yazbek, W., Pré, P., & Delebarre, A. (2006). Adsorption and Desorption of Volatile Organic Compounds in Fluidized Bed. *Journal of Environmental Engineering, 132*, 442-452.

Yihong, Q., Chen, Y., Zhang, G. G., Yu, L., & Mantri, R. V. (2017). *Developing Solid Oral Dosage Forms.* Mica Haley.

Yu, S., Li, X., Liu, S., Hao, J., Shao, Z., & Yi, B. (2014). Study on hydrophobicity loss of the gas diffusion layer in PEMFCs by electrochemical oxidation. *The Royal Society of Chemistry, 4*, 3852–3856.

Zaitan, H., Manero, M. H., & Valdes, H. (2016). Application of high silica zeolite ZSM-5 in a hybrid treatment process based on sequential adsorption and ozonation for VOCs elimination. *Journal of Environmental Sciences, 41*, 59-68.

Zhang, X., Gao, B., Creamer, A., Cao, C., & Li, Y. (2017). Adsorption of VOCs onto engineered carbon materials: A review. *Journal of Hazardous Materials*, 102-123.

Zhou, L., Chen, Y.-L., Zhang, X.-H., Tian, F.-M., & Zu, Z.-N. (2014). Zeolites developed from mixed alkali modified coal fly ash for adsorption of volatile organic compounds. *Materials Letters, 119*, 140–142.

Zhu, L., Shen, D., & Luo, K. H. (2020). A critical review on VOCs adsorption by different porous materials: Species, mechanisms and modification methods. *Journal of Hazardous Materials, 389*, 122102.